Prepared for:

Rijkswaterstaat, Dienst Getijdewateren

Coastal Genesis Project

Sediment transport, sediment concentrations and bedforms in simulated asymmetric wave conditions

Experimental study in the large oscillating water tunnel of DELFT HYDRAULICS

Data-report, H 840.20, Part V

April 1992

delft hydraulics

Sediment transport, sediment concentrations and bedforms in simulated asymmetric wave conditions

Experimental study in the large oscillating water tunnel of
DELFT HYDRAULICS

Jan S. Ribberink and Abdullah Al-Salem

delft hydraulics

ABSTRACT

Near-bed sediment transport phenomenae were studied in simulated asymmetric wave conditions at full scale (1:1) in the Large Oscillating Water Tunnel of DELFT HYDRAULICS.

As a follow-up of a first set of experiments (see Ribberink and Al-Salem, 1991) eight experiments were conducted with regular asymmetric waves (exp's 13-16) and irregular asymmetric waves (exp's 17-20) in which measurements of bed forms, suspended sediment concentrations and net sediment transport rates were carried out.

The specific objectives of the measurements (series B: exp's 1-20) were:

- to study the near-bed sediment transport phenomenae in the low-velocity regime (transition to rippled-bed conditions),
- to study the effects of the wave-period and degree of wave-asymmetry,
- to obtain data for the verification and development of various types of models for the near-bed sediment behaviour.

This report is a data-report in which the rough data and only a limited data-analysis are presented.

The main results are:

- The vortex-development and convection in rippled-bed conditions has a large influence on the near-bed sediment dynamics (suspended sediment load and net sediment transport rate).
- In the transition regime from rippled-bed to plane-bed conditions an increasing near bed-velocity first leads to a reduction in suspended load (reduced vertical mixing induced by vortices) but is then followed by an increase in suspended load in plane-bed conditions (increased turbulent mixing).
- The measured net sediment transport rates as induced by the asymmetry were all in the direction of the wave propagation and showed a consistent linear relation with the third- order moment of the velocity $\langle U^3 \rangle$ in plane-bed and small rippled-bed conditions. The different degree of asymmetry of the waves did not influence the relation.
- For larger ripples the measured net transport rates were still in the direction of the wave propagation but considerably lower than according to the above mentioned $\langle U^3 \rangle$ relation (effect of vortex-development/convection).
- The effect of the wave-period appeared to be important, especially in rippled-bed conditions.

CONTENTS

LIST OF TABLES

LIST OF FIGURES

MAIN SYMBOLS

C	Sediment concentration in dry weight per unit of volume
$\langle C \rangle$	Time-averaged sediment concentration
C_0	Sediment bed concentration ($z = 0$) determined graphically from the measured concentration profiles
D_{50}	Median sediment size
d_0	Stroke of the oscillatory water motion ($= 2\hat{x}$)
ϵ_0	Porosity of sand
f_w	Wave friction factor
T	Period of the oscillatory motion
$\tilde{U}$	Instantaneous horizontal velocity
U_c	Maximum velocity during the 'onshore' directed half cycle (crest)
U_t	Maximum velocity during the 'offshore' directed half cycle (trough)
U_{rms}	Root mean square value of the horizontal velocity
λ	Ripple length
η	Ripple height
ρ_s	Density of sediment
ρ	Density of water
ψ	Mobility number $(= \frac{\hat{U}^2}{\Delta g D_{50}})$
ψ_c	Mobility number based on U_c
ψ_t	Mobility number based on U_t
Δ	Relative sand density $(= \frac{\rho_s - \rho}{\rho})$
Θ	Dimensionless bed shear stress $(= \frac{1}{2} f_w \psi)$
$\langle q_s \rangle$	Time-averaged (net) sediment transport rate (expressed in sediment volume per unit time and width)
R	Degree of asymmetry $(= \frac{U_c}{(U_c + U_t)})$
$\hat{x}$	Amplitude of the oscillatory water motion

1. Introduction

The sediment transport processes under sea waves are substantially influenced by the non-linearity (e.g. wave asymmetry) and randomness of the wave motion. Especially on the upper shoreface but also in the surf zone wave asymmetry appears to be an important driving mechanism for the transport of sediment in (generally) cross-shore direction and can often be held responsible for onshore motion of offshore bars.

For an extensive description of the phenomenon "wave-asymmetry induced sediment transport" and of the research in the oscillating water tunnel reference is made to Ribberink and Al-Salem (1991).
A first set of experiments (exp's B1-B12) was described which were especially aimed at the behaviour of the net transport, suspended sediment concentrations and bedforms in asymmetric wave conditions. During all the tests the bed was (almost) plane and the measured net transport rates showed a consistent linear relation with the velocity moment $\langle U^3 \rangle$ (i.e. the time-averaged value of the third power of the near-bed horizontal velocity above the wave boundary layer). The measurements also showed a reasonable agreement (within a factor 2) with the transport formulae of Bailard (1981). A systematic effect of the wave period (20-60% larger transport rates for T = 9.1 s instead of T = 6.5 s) could not be explained by this model, which neglects several types of phase-lag effects and acceleration effects in the wave boundary layer.

The experiments as described in the present report (exp's B13-B20) are the follow-up of the series B experiments as described above. In order to learn more about the validity of the "Bailard type" transport formulae concept:

- the lower velocity regime was entered in which a transition to rippled beds could be expected,
- specific experiments were carried out aimed at the effects of the wave period and the degree of wave-asymmetry.

The present report contains the measured data (data report) and a limited data-analysis.

This work was undertaken as part of the Coastal Genesis research programme. It was funded by the Ministry of Transport and Public Works in the Netherlands (Rijkwaterstaat, Tidal Waters Division). The measurements were carried out by Mr. H. Westhuis and Mr. T. van Maar. Analysis and reporting were carried out by Mr. A. Al-Salem and Mr. J.S. Ribberink.

2. Experimental set-up

2.1 Experimental facility and measuring techniques

An extensive description of the DH large oscillatory water tunnel is given by Ribberink (1989).

Figure 2.1 gives a general impression of the imposed and measured parameters during the present experiments. The following measuring techniques were used during each experimental run:

- A laser doppler system was used for measuring the horizontal and vertical water velocity components. It was positioned in the middle of the test section at a height of 20 cm above the bed (above the wave-boundary layer).
- A transverse suction technique was used for measuring the time-averaged concentration profiles of suspended sediment near the bed (1-15 cm).
- A mass-conservation technique was used for measuring the net transport rate. It was measured indirectly by numerical integration of the sediment-continuity equation using bed-level changes along the test section and collected sand volumes in the two sand traps.

For more detailed information about the techniques, see Ribberink and Al-Salem (1991).

2.2 Experimental procedure

The following experimental procedure was followed during each experimental run:

- flatten the bed,
- measure the initial bed level along the test section (13 meters, space-step, Δx = 10 cm),
- position the measuring instruments above the bed,
- set the required piston position amplitude and then start the experiment by activating the PC steering/data-acquisition system (l.d.a signal),
- measure height, length and travelling speed of the ripples through the glass window at three positions along the test section (left, right and middle) for every 10 minutes after reaching steady-state conditions.
- measure the time-averaged sediment concentration profiles with the transverse suction technique (15 min each measurement),

- stop the tunnel after the test run is completed,
- measure the bed level again,
- empty the two sand traps and weigh the sand under water.

Remark

For some rippled-bed experiments the influence of using different space-steps (Δx = 2.5, 5.0 and 10.0 cm) for the bed-level measurements (mass-conservation technique) was tested but no significant effect on the measured transport rate was observed.
Moreover, the bed level was measured along the other side of the test section but again no significant effect was found.

2.3 Test programme

The experiments were carried out with regular and irregular asymmetric oscillatory flow. The 2nd-order Stokes wave theory was used for simulating the regular asymmetric waves. A JONSWAP spectrum for the wave motion in combination with a 2nd-order wave theory (Liu and Dingemans, 1989) was applied for the simulation of the irregular asymmetric waves. The experiments were carried out with quartz sand (unsorted dune sand). Figure 2.2 shows the grain-size distribution (D_{10} = 0.15 mm, D_{50} = 0.21 mm, D_{90} = 0.29 mm).

The main objectives were:
- testing the influence of the wave-period T on the transport process (T = 5-12 s),
- testing the influence of the degree of wave-asymmetry on the transport process,
- testing the influence of bed ripples on the transport process (more dominant suspended load and phase-lag effects),
- to obtain data for the verification and development of various type of models for the near-bed sediment behaviour, e.g. testing the validity of the empirical power-law description for the transport rate ($\langle q_s \rangle \sim \langle U^3 \rangle$).

During a first set of 2 experiments (exp's B13 and B14) two previous experiments with regular asymmetric waves (exp's B8 and B11, U_{rms} = 0.7 m/s, T = 6.5 and 9.1 s) were repeated with a lower degree of asymmetry. The degree of asymmetry R is defined as the ratio of the (significant) crest velocity and the sum

of the (significant) crest and trough velocity of the horizontal wave orbital motion.

During a second set of 2 experiments (exp's B15 and B16) with regular asymmetric waves two different wave periods (5, 12 s) were applied in combination with U_{rms} = 0.52 m/s and the "normal" degree of asymmetry.

During the third set of 4 experiments (exp's B17 ... B20) the low-velocity regime was entered (U_{rms} = 0.20 - 0.25 m/s), with irregular asymmetric waves and wave periods in the range T = 5 - 9.1 s.

For more information about the experimental conditions of all 20 experiments (series B), see Table 2.1.

3. Experimental results and analysis

3.1 Sediment transport rate

The sediment transport was directed 'onshore' (i.e. in the direction of the wave propagation) for all the plane- and rippled-bed experiments. The measured transport rates for all the tests are summarized in Tables 3.1-3.8. Two estimates were obtained for the transport rate in the middle of the test section (by using the left and right sand traps, see Appendix C in Ribberink and Al-Salem, 1991). The Figures 3.1-3.4 show the distribution of the two computed estimates of the net transport rate (without pores per unit width) along the test section.

The measured net transport rates show a very consistent relation with the time-averaged value of the third power of the instantaneous velocity $\langle U^3 \rangle$. Figure 3.5 shows this relation for all experiments with periods 6.5 s and 9.1 s (plane bed and rippled bed). The experiments with a different degree of asymmetry (exp's B13 and B14) fitted well in the relation. Only one experiment in the rippled-bed regime, viz. exp. B17 with the largest ripples and the lowest U_{rms}, showed a clear reduction of the net transport rate. This can be explained by the increased importance of an offshore-directed transport component as induced by the large ripples (vortex development and convection).

The Figures 3.6 and 3.7 show that the fourth and sixth power of the velocity do not give a linear relation with the measured net transport rate.

The influence of the wave period (for constant U_{rms}) is shown in Fig. 3.8, in the ripple bed regime (U_{rms} = 0.25 m/s) and in the plane bed regime (U_{rms} = 0.5 m/s). The net transport rate generally increases for increasing period. In rippled bed conditions again the strong dependence of the ripple-dimensions (= period dependent) becomes clear.

In Table 3.9 the main results of the experiments (series B) are summarized.

Remark: In this table the (skin) friction factor f_w' based on Jonsson's (1980) formulation is added. In this formula the roughness height was chosen as $k_s = D_{50}$ (see also Ribberink and Al-Salem, 1991). For the "irregular wave" experiments the significant value of the amplitude of the

oscillatory water motion was used ($\hat{x} = \hat{x}_{sig}$). The skin friction factor can be applied for the transformation of velocity to bed-shear stress (skin friction). The latter can be used as an input parameter for transport formulations.

3.2 Time-averaged sediment concentrations

The concentration profiles as measured with the suction system are summarized in the Tables 3.10 ... 3.23. For each experiment 5-10 different suction measurements were carried out.
Figure 3.9 shows the influence of the type of oscillatory flow (irregularity) in the low-velocity regime (rippled bed) and in the high-velocity regime (plane bed). In rippled-bed conditions the regular/sinusoidal oscillatory flow generates larger vortex ripples than irregular/asymmetric oscillatory flow. This leads to an increased vertical mixing and an increased suspended load for the regular sinusoidal case. This influence was minor for the plane-bed regime, in which the concentration profiles seem to be fully determined by the root mean square of the horizontal velocity (U_{rms}).

Figure 3.10 shows that, for a constant type of irregularity and a constant wave period, the influence of U_{rms} is opposite in rippled bed and plane-bed conditions. In plane-bed conditions an increase in U_{rms} leads to an increase in bed-shear stress, an increased turbulent mixing and an increased suspended load. In rippled-bed conditions the decrease in U_{rms} causes an increase in the ripple dimensions (transition plane bed to ripples) and leads simultaneously to an increased vertical mixing and more suspended load.

Figure 3.11 shows the influence of the wave period on the concentration profiles in both bed regimes. In plane-bed conditions no period influence could be observed for a constant U_{rms} = 0.5-0.55 m/s. In rippled-bed conditions the larger periods lead to a decrease of ripple dimensions and suspended load (constant U_{rms} = 0.25 m/s).

Figure 3.12 shows the influence of the degree of asymmetry R on the concentration profiles for plane-bed conditions and two wave-periods (6.5 s and 9.1 s). For the low-period case (6.5 s) the higher asymmetry caused some increase in suspended load. No influence was observed for the large wave period 9.1 s.

In the Figures 3.13-3.22 the measured time-averaged concentration profiles for all the series B experiments (exp's B1-B20) are plotted on log-log x-y scales. An almost constant slope was observed for all the plane-bed and the small rippled-bed experiments (exp's B1-B16: slope $\alpha = 2.1 \pm 5\%$, see Table 3.24). For the other rippled-bed experiments (exp's B17-B20) the slope varied along the vertical and a better (linear) fit was obtained with a log-linear x-y scale (see Figures 3.23 and 3.24).

As a consequence the following power-law distribution can be applied for the description of the concentration profile in plane-bed conditions:

$$C(z) = C_a \, (z_a/z)^{\alpha}$$

with:
C_a = a reference concentration at level $z = z_a$
$\alpha = 2.1$

For rippled-bed conditions the well-known negative exponential distribution (see e.g. Bosman and Steetzel, 1986) shows the best behaviour:

$$C(z) = C_0 \exp(-z/r_c)$$

with:
C_0 = (extrapolated) concentration at $z = 0$ (= average bed level)
r_c = concentration decay length.

In Table 3.24 the measured values of C_0 and r_c are listed.

3.3 Bed-form geometry

In the low-velocity regime bed ripples were formed ($U_{rms} < 0.35$ m/s). Small-scale ripples developed at the beginning of the ripple formation from initially flat bed. The scale of ripples continued to grow by the action of vortices formed on the lee side of ripples. It generally required 10 to 15 minutes until steady-state ripples were present.

The Figures 3.25 and 3.26 show the measured ripple height and length as a function U_{rms} for all 20 series B experiments. It can be seen that for increasing U_{rms} ripple heights and length tend to decrease until plane bed is reached.

Table 3.25 gives the measured values of the ripple height, length, speed and gives information about the type of bed forms (2D/3D/plane bed).

3.4 Specific phenomenae

- During all experiments vertical sorting of sediments took place. The finer size fractions are suspended more easily than the coarse fractions and consequently the concentration profiles consist of relatively fine sand at higher levels.
  Figure 3.27 shows the measured variation of D_{50} along the vertical for experiment B18 (as obtained from the suction samples). Figure 3.28 shows the measured (time-averaged) concentration profile of individual size fractions during the same experiment.
- Small (secondary) net currents are generated by the (asymmetric) oscillatory flow in the tunnel. Above the wave boundary layer the direction of the net current is generally "onshore". Closer to the sand bed a compensating net flow in "offshore" direction is generally observed.
  Figure 3.30 shows two measured net current-velocity profiles $\langle U(z) \rangle$ (exp's B10 and B17). Multiplied with the time-averaged concentration profile $\langle C(z) \rangle$, the current-related sediment flux profile can be obtained (see Fig. 3.30). It can be seen that for both experiments a negative (offshore directed) sediment flux takes place close to the bed. The contribution of this current-related suspended sediment to the measured total (wave + current related) net sediment transport (see Table 3.9) is small (5-15%).
- In close connection with the vertical sorting process also the longitudinal sorting of sediment took place (along the tunnel test section).
  Figure 3.29 shows the measured variation of D_{50} (bed sediment) along the test section of the tunnel for experiment B18. The net transport direction is from left to right (= direction of the "wave propagation" = "onshore"). Especially the coarse size fractions are transported to the right by the wave-asymmetry. The D_{50}-value of the sand collected in the right sand trap is also considerably larger than in the left trap.
  Finer size fractions have a preference to be transported to the left ("offshore") by the net current close to the bed.

REFERENCES

Bosman, J.J. and Steetzel, H.J., (1986).
Time and bed averaged concentration under waves.
Proc. 20th Int. Coast. Eng. Conf., Taipeh, November.

Ribberink, J.S., (1989).
The large oscillating water tunnel.
Technical specifications and performances.
DELFT HYDRAULICS, Report No. H840, Part 1, March.

Ribberink, J.S. and Al-Salem A., (1991).
Sediment transport, sediment concentrations and bedforms in simulated asymmetric wave conditions.
DELFT HYDRAULICS, Report No. H840, Part 4, February.

Exp.	T_p (s)	U_{rms} (m/s)	Type of oscillating flow		Test duration			Total no. of tests
			Asymmetry (-)	Regular/irregular	hr	min	sec	
B1	6.5	0.48	0.61-0.62	irregular, JONSWAP 2nd order Stokes	00	36	00	12
B2	6.5	0.32			00	12	00	12
B3	6.5	0.43			01	12	00	8
B4	9.1	0.48			00	50	25	8
B5	9.1	0.33			01	40	50	8
B6	9.1	0.44			01	40	50	6
B7	6.5	0.50	0.64-0.67	regular 2nd order Stokes	00	20	00	6
B8	6.5	0.70			00	10	00	7
B9	6.5	0.92			00	05	00	6
B10	9.1	0.54			00	28	00	10
B11	9.1	0.70			00	14	00	5
B12	9.1	0.97			00	07	00	5
B13	6.5	0.70	0.57		00	45	30	6
B14	9.1	0.71	0.56		00	25	00	9
B15	5.0	0.51	0.64		00	25	00	6
B16	12.0	0.56	0.62		00	20	00	7
B17	6.5	0.20	0.61-0.63	irregular, JONSWAP 2nd order Stokes	15	00	00	3
B18	6.5	0.25			06	00	00	5
B19	5.0	0.25			07	30	00	5
B20	9.1	0.25			03	00	00	5

Table 2.1 Experimental conditions

Experiment B13

Test	Dry collected sand weight in traps (kg)			Change of sand volume in test section (10^{-3} m^3)			$1-\epsilon_0$	q_{SL} (10^{-6} m^2/s)	q_{SR} (10^{-6} m^2/s)	q_{Savg} (10^{-6} m^2/s)
	Left	Right	Total	$\Delta V_{l_{ip}}$	$\Delta V_{r_{ip}}$	Total				
13.1	4.66	15.73	20.39	+31.5	-14.1	+17.4	0.44	22.1	18.1	20.1
13.3	5.30	15.25	20.55	+33.7	-14.1	+19.6	0.40	23.5	17.9	20.7
13.4	3.53	15.41	18.94	+32.0	-15.5	+16.5	0.43	23.0	19.1	21.1
13.5	5.62	11.40	17.02	+33.2	-22.3	+10.93	0.59	23.0	22.4	22.7

21.14 ± 2.43 (11.5%, 5.75%)
$q_s \pm \sigma(r = \frac{\sigma}{q_s}, \frac{r}{\sqrt{N}})$

Table 3.1 Measured transport rates

Experiment B14

Test	Dry collected sand weight in traps (kg)			Change of sand volume in test section (10^{-3} m^3)			$1-\epsilon_0$	q_{SL} (10^{-6} m^2/s)	q_{SR} (10^{-6} m^2/s)	q_{Savg} (10^{-6} m^2/s)
	Left	Right	Total	$\Delta V_{l_{ip}}$	$\Delta V_{r_{ip}}$	Total				
14.2	1.77	3.53	5.30	+ 17.7	- 6.7	+ 11.0	0.18	29.1	15.4	22.3
14.3	2.41	4.65	7.10	+ 21.0	- 13.9	+ 7.1	0.37	27.4	23.3	25.3
14.4	2.25	4.33	6.58	+ 20.4	- 15.1	+ 5.3	0.47	26.7	24.7	25.7
14.5	2.25	4.81	7.10	+ 19.9	- 9.4	+ 10.5	0.26	26.0	17.2	21.6
14.6	2.41	4.17	6.58	+ 21.3	- 8.6	+ 12.7	0.20	27.8	15.6	21.6
14.7	3.37	4.25	7.62	+ 18.3	- 9.6	+ 8.6	0.33	22.7	17.0	19.9
14.8	3.21	4.33	7.54	+ 20.3	- 9.2	+ 11.1	0.27	25.7	16.5	21.1
14.9	2.89	3.85	6.74	+ 17.42	- 11.44	+ 5.98	0.43	21.97	19.24	20.61
										21.98 ± 4.52 (20.6%, 7.3%)

Table 3.2 Measured transport rates

Experiment B15

Test	Dry collected sand weight in traps (kg)			Change of sand volume in test section (10^{-3} m^3)			$1-\epsilon_0$	q_{SL} (10^{-6} m^2/s)	q_{SR} (10^{-6} m^2/s)	q_{Savg} (10^{-6} m^2/s)
	Left	Right	Total	$\Delta V_{l_{ip}}$	$\Delta V_{r_{ip}}$	Total				
15.1	0.24	9.47	9.71	+ 13.4	- 6.07	+ 7.33	0.50	18.55	16.59	17.57
15.2	0.16	8.03	8.19	+ 13.6	- 4.2	+ 9.4	0.33	18.82	12.74	15.78
15.3	0.32	6.23	6.55	+ 11.2	- 4.4	+ 6.8	0.36	15.38	11.45	13.42
15.4	0.64	6.90	7.54	+ 14.1	- 4.2	+ 9.9	0.29	19.21	11.75	15.48
15.5	0.40	7.54	7.94	+ 11.3	- 5.6	+ 5.7	0.53	15.46	14.27	14.87
15.6	0.40	11.27	11.67	+ 9.80	- 3.74	+ 6.07	0.73	13.38	14.86	14.12
										15.21 ± 2.49 (16.4%, 6.7%)

Table 3.3 Measured transport rates

Experiment B16

Test	Dry collected sand weight in traps (kg)			Change of sand volume in test section (10^{-3} m^3)			$1-\epsilon_0$	q_{SL} (10^{-6} m^2/s)	q_{SR} (10^{-6} m^2/s)	q_{Savg} (10^{-6} m^2/s)
	Left	Right	Total	$\Delta V_{l_{ip}}$	$\Delta V_{r_{ip}}$	Total				
16.1	0.40	9.31	9.71	+ 9.29	- 3.32	+ 5.98	0.61	19.0	19.0	19.0
16.2	0.32	8.99	9.31	+ 11.61	- 6.43	+ 5.18	0.68	20.0	21.0	20.5
16.3	0.48	8.83	9.31	+ 12.08	- 6.03	+ 6.05	0.58	20.0	21.0	20.5
16.4	0.40	8.19	8.59	+ 8.30	- 3.46	+ 4.84	0.67	16.0	17.0	16.5
16.5	0.40	10.11	10.51	+ 11.19	- 6.89	+ 4.30	0.92	19.0	23.0	21.0
16.6	0.40	8.19	8.59	+ 15.26	- 7.35	+ 7.91	0.41	26.0	22.0	24.0
16.7	0.48	8.03	8.51	+ 9.68	- 5.07	+ 4.61	0.70	16.5	17.5	17.0
										19.79 ± 1.34 (6.8%, 2.6%)

Table 3.4 Measured transport rates

Experiment B17

Test	Dry collected sand weight in traps (kg)			Change of sand volume in test section (10^{-3} m^3)			$1-\epsilon_o$	q_{SL} (10^{-6} m^2/s)	q_{SR} (10^{-6} m^2/s)	q_{Savg} (10^{-6} m^2/s)
	Left	Right	Total	$\Delta V_{l_{ip}}$	$\Delta V_{r_{ip}}$	Total				
17.1	1.61	34.27	35.88	+ 7.64	+ 16.04	+ 23.68	0.57	0.25	0.18	0.21
17.2	1.45	32.10	33.55	+ 7.52	+ 10.46	+ 17.98	0.70	0.26	0.36	0.31
17.3	0.96	32.42	33.38	+ 6.41	+ 12.74	+ 19.14	0.66	0.23	0.28	0.25
										0.26 ± 0.035 (13.5%, 7.8%)

Table 3.5 Measured transport rates

Experiment B18

Test	Dry collected sand weight in traps (kg)			Change of sand volume in test section (10^{-3} m^3)			$1-\epsilon_0$	q_{SL} (10^{-6} m^2/s)	q_{SR} (10^{-6} m^2/s)	q_{Savg} (10^{-6} m^2/s)
	Left	Right	Total	$\Delta V_{l_{ip}}$	$\Delta V_{r_{ip}}$	Total				
18.1	1.45	36.43	37.88	+ 12.68	- 0.09	+ 12.59	1.14	1.15	2.17	1.66
18.2	1.61	34.67	36.28	+ 16.49	- 4.23	+ 12.26	1.12	1.51	2.49	2.0
18.3	2.01	37.24	39.25	+ 20.82	- 0.11	+ 20.71	0.72	1.91	2.22	2.06
18.4	1.61	39.0	40.61	+ 16.95	- 2.0	+ 14.95	1.02	1.55	2.51	2.03
18.5	2.09	35.31	37.40	+ 25.11	- 2.49	+ 22.62	0.62	2.31	2.34	2.33
										2.02 ± 0.45 (22.3%, 10%)

Table 3.6 Measured transport rates

Experiment B19

Test	Dry collected sand weight in traps (kg)			Change of sand volume in test section (10^{-3} m^3)			$1-\epsilon_0$	q_{SL} (10^{-6} m^2/s)	q_{SR} (10^{-6} m^2/s)	q_{Savg} (10^{-6} m^2/s)
	Left	Right	Total	$\Delta V_{l_{ip}}$	$\Delta V_{r_{ip}}$	Total				
19.1	2.49	27.29	29.78	+ 0.49	+ 11.46	+ 11.95	0.94	0.08	0.40	0.24
19.2	1.61	24.88	26.49	+ 3.35	+ 14.97	+ 18.32	0.55	0.19	0.01	0.10
19.3	1.77	21.99	23.76	+ 2.40	+ 8.28	+ 10.68	0.84	0.104	0.38	0.24
19.4	1.28	26.96	28.25	+ 9.90	+ 10.44	+ 20.34	0.52	0.71	0.44	0.58
19.5	1.45	31.78	33.22	+ 9.72	+ 6.86	+ 16.58	0.76	0.69	0.98	0.83
										0.40 ± 0.27 (67.5%, 30.2%)

Table 3.7 Measured transport rates

Experiment B20

Test	Dry collected sand weight in traps (kg)			Change of sand volume in test section (10^{-3} m^3)			$1-\epsilon_0$	q_{SL} (10^{-6} m^2/s)	q_{SR} (10^{-6} m^2/s)	q_{Savg} (10^{-6} m^2/s)
	Left	Right	Total	$\Delta V_{l_{ip}}$	$\Delta V_{r_{ip}}$	Total				
20.1	0.72	19.26	19.98	+ 15.62	- 1.59	+ 14.03	0.54	2.95	2.60	2.80
20.1	0.80	21.51	22.31	+ 15.69	- 0.13	+ 15.56	0.54	2.96	2.58	2.77
20.3	0.64	18.62	19.26	+ 14.74	- 1.22	+ 13.52	0.54	2.79	2.45	2.62
20.4	0.80	21.67	22.47	+ 13.54	- 2.15	+ 11.39	0.75	2.54	2.94	2.74
20.5	0.96	21.83	22.79	+ 15.42	- 3.09	+ 12.33	0.70	2.89	3.14	3.02
										2.79 ± 0.14 (5%, 2.2%)

Table 3.8 Measured transport rates

Irregular asymmetric (random) waves

Experiment no.	U_{rms} (m/s)	T_p (s)	$U_{c(sig)}$ (m/s)	$U_{t(sig)}$ (m/s)	$\langle U \rangle$ (cm/s)	Degree of asymmetry R = $U_c/(U_c+U_t)$	$x_{(sig)}$ (m)	f'_w ($1.0E^{-3}$)	ψ_c	ψ_t	θ_c	θ_t	Velocity moments $\langle U^3 \rangle$ m^3/s^3	Velocity moments $\langle \lvert U \rvert^3 U \rangle$ m^4/s^4	Velocity moments $\langle \lvert U \rvert^5 U \rangle$ m^6/s^6	$\langle q_s \rangle$ $1.0E^{-6}$ m^2/s	λ (cm)	η (cm)
1	0.48	6.5	1.20	0.73	0.8	0.62	0.86	7.12	423.6	156.8	1.51	0.56	0.074	0.105	0.206	12.26	-	-
2	0.32	6.5	0.80	0.52	-0.3	0.61	0.56	7.80	188.3	79.5	0.73	0.31	0.019	0.019	0.018	3.27	8.7	0.35
3	0.43	6.5	1.08	0.70	-1.6	0.61	0.76	7.32	343.1	144.2	1.25	0.53	0.046	0.062	0.102	8.04	-	-
4	0.48	9.1	1.17	0.73	0.1	0.62	1.20	6.68	402.7	156.8	1.35	0.52	0.067	0.095	0.191	14.61	-	-
5	0.33	9.1	0.79	0.49	0.05	0.62	0.81	7.22	183.6	70.6	0.66	0.25	0.021	0.021	0.020	4.14	8.4	0.3
6	0.44	9.1	1.11	0.70	-2.4	0.61	1.10	6.80	362.5	144.2	1.23	0.49	0.037	0.053	0.095	11.96	-	-

Regular asymmetric waves

Experiment no.	U_{rms} (m/s)	T_p (s)	$U_{c(sig)}$ (m/s)	$U_{t(sig)}$ (m/s)	$\langle U \rangle$ (cm/s)	Degree of asymmetry R = $U_c/(U_c+U_t)$	$x_{(sig)}$ (m)	f'_w ($1.0E^{-3}$)	ψ_c	ψ_t	θ_c	θ_t	Velocity moments $\langle U^3 \rangle$ m^3/s^3	Velocity moments $\langle \lvert U \rvert^3 U \rangle$ m^4/s^4	Velocity moments $\langle \lvert U \rvert^5 U \rangle$ m^6/s^6	$\langle q_s \rangle$ $1.0E^{-6}$ m^2/s	λ (cm)	η (cm)
7	0.50	6.5	0.95	0.50	4.8	0.66	0.67	7.50	265.5	73.5	1.0	0.28	0.102	0.096	0.075	12.42	-	-
8	0.70	6.5	1.31	0.70	3.8	0.65	0.93	7.02	504.9	144.2	1.77	0.51	0.256	0.343	0.536	38.85	-	-
9	0.92	6.5	1.72	0.86	3.0	0.67	1.21	6.66	870.3	217.6	2.90	0.72	0.562	0.998	2.700	69.83	-	-
10	0.54	9.1	0.96	0.53	2.0	0.64	1.01	6.90	271.1	82.6	0.94	0.29	0.104	0.106	0.093	18.56	-	-
11	0.70	9.1	1.25	0.69	2.2	0.64	1.34	6.54	459.7	140.1	1.50	0.46	0.220	0.294	0.442	44.83	-	-
12	0.97	9.1	1.75	0.99	2.9	0.64	1.86	6.20	901.0	288.3	2.79	0.89	0.574	1.062	3.062	120.88	-	-

Table 3.9 Summary of measuring results, experiment series B

Regular asymmetric (random waves)

Experiment no.	U_{rms} (m/s)	T_p (s)	$U_{c(sig)}$ (m/s)	$U_{t(sig)}$ (m/s)	Degree of asymmetry $R = U_c/(U_c+U_t)$	$x_{(sig)}$ (m)	f'_w (10^{-3})	ψ_c	ψ_t	θ_c	θ_t	Velocity moments						$\langle q_s \rangle$ 10^{-6} m^2/s	λ (cm)	η (cm)
												$\langle U \rangle$ m/s	$\langle \lvert U \rvert U \rangle$ m^2/s^2	$\langle U^3 \rangle$ m^3/s^3	$\langle \lvert U \rvert^3 U \rangle$ m^4/s^4	$\langle \lvert U^5 \rangle$ m^5/s^5	$\langle \lvert U^5 \rvert U$ m^6/s^6			
13	0.70	6.5	1.20	0.90	0.57	0.94	7.0	424	238	1.48	0.83	0.010	0.069	0.114	0.151	-	0.217	21.1	-	-
14	0.71	9.1	1.19	0.92	0.56	1.34	6.5	417	249	1.36	0.81	-0.064	0.051	0.094	0.133	-	0.198	22.0	-	-
15	0.51	5.0	0.98	0.54	0.64	0.54	7.9	283	86	1.12	0.34	0.030	0.089	0.103	0.102	-	0.087	15.2	-	-
16	0.56	12.0	1.03	0.63	0.62	1.42	6.5	312	117	1.01	0.38	0.005	-	0.101	0.109	-	0.105	19.8	-	-

Irregular asymmetric (random waves)

Experiment no.	U_{rms} (m/s)	T_p (s)	$U_{c(sig)}$ (m/s)	$U_{t(sig)}$ (m/s)	Degree of asymmetry $R = U_c/(U_c+U_t)$	$x_{(sig)}$ (m)	f'_w (10^{-3})	ψ_c	ψ_t	θ_c	θ_t	Velocity moments						$\langle q_s \rangle$ 10^{-6} m^2/s	λ (cm)	η (cm)
												$\langle U \rangle$ m/s	$\langle \lvert U \rvert U \rangle$ m^2/s^2	$\langle U^3 \rangle$ m^3/s^3	$\langle \lvert U \rvert^3 U \rangle$ m^4/s^4	$\langle \lvert U^5 \rangle$ m^5/s^5	$\langle \lvert U^5 \rvert U$ m^6/s^6			
17	0.20	6.5	0.44	0.28	0.61	0.36	8.6	57	23	0.25	0.10	0.0062	0.0091	0.0058	0.0034	0.0021	0.0013	0.26	11	1.43
18	0.25	6.5	0.64	0.37	0.63	0.46	8.1	121	40	0.49	0.16	0.0051	0.0145	0.0127	0.0101	0.0081	0.0068	2.02	9	0.90
19	0.25	5.0	0.66	0.39	0.63	0.36	8.6	128	45	0.55	0.19	0.0051	0.0162	0.0149	0.0129	0.0110	0.0101	0.38	9.8	1.12
20	0.25	9.1	0.60	0.38	0.61	0.67	7.5	106	43	0.40	0.16	-0.0011	0.0121	0.0121	0.0106	0.0096	0.0091	2.79	9.1	0.71

Table 3.9 Summary of measuring results, experiment series B (continued)

B13.1

Z (cm)	<C>(g/l)	Z (cm)	<C>(g/l)
1.6	1.320	2.2	0.790
2.6	0.378	3.2	0.270
3.6	0.176	4.2	0.110
5.1	0.099	5.7	0.050
7.1	0.043	7.7	0.020
9.1	0.022	9.7	0.010

B13.2

Z (cm)	<C>(g/l)	Z (cm)	<C>(g/l)
0.9	3.959	0.7	4.361
1.9	0.777	1.7	0.731
2.9	0.327	2.7	0.292
4.4	0.150	4.2	0.131
6.4	0.075	6.2	0.055
8.4	0.026	8.2	0.020

B13.3

Z (cm)	<C>(g/l)	Z (cm)	<C>(g/l)
1.5	0.789	1.0	3.441
2.5	0.241	2.0	0.783
3.5	0.104	3.0	0.312
5.0	0.045	4.5	0.149
7.0	0.020	6.5	0.058
9.0	0.006	8.5	0.020

B13.4

Z (cm)	<C>(g/l)	Z (cm)	<C>(g/l)
1.0	3.515	1.0	3.619
2.0	0.808	2.0	0.826
3.0	0.325	3.0	0.345
4.5	0.158	4.5	0.162
6.5	0.064	6.5	0.070
8.5	0.022	8.5	0.024

Table 3.10 Measured vertical concentration distributions

B13.5

Z (cm)	<C>(g/l)	Z (cm)	<C>(g/l)
1.0	4.450	0.9	4.820
2.0	0.937	1.9	1.109
3.0	0.384	2.9	0.481
4.5	0.189	4.4	0.234
6.5	0.081	6.4	0.101
8.5	0.024	8.4	0.035

B13.6

Z (cm)	<C>(g/l)	Z (cm)	<C>(g/l)
0.8	3.190	0.6	3.980
1.8	0.671	1.6	0.706
2.8	0.267	2.6	0.247
4.3	0.131	4.1	0.135
6.3	0.055	6.1	0.060
8.3	0.022	8.1	0.026

B14.1

Z (cm)	<C>(g/l)	Z (cm)	<C>(g/l)
0.6	4.580	0.5	4.038
1.6	1.612	1.5	1.676
2.6	0.591	2.5	0.683
4.1	0.270	4.0	0.311
6.1	0.128	6.0	0.137
8.1	0.050	8.0	0.071

B14.2

Z (cm)	<C>(g/l)
1.0	4.036
2.0	1.161
3.0	0.507
4.5	0.248
6.5	0.104
7.5	0.043

Table 3.11 Measured vertical concentration distributions

B14.3

Z (cm)	<C>(g/l)	Z (cm)	<C>(g/l)
1.0	3.526	0.6	6.078
2.0	0.937	1.6	1.472
3.0	0.429	2.6	0.569
4.5	0.198	4.1	0.268
6.5	0.087	6.1	0.115
8.5	0.050	8.1	0.051

B14.4

Z (cm)	<C>(g/l)
1.0	3.434
2.0	1.307
3.0	0.494
4.5	0.257
6.5	0.113
8.5	0.044

B14.5

Z (cm)	<C>(g/l)
0.9	3.619
1.9	1.187
2.9	0.507
4.4	0.248
6.4	0.107
8.4	0.050

B14.6

Z (cm)	<C>(g/l)
1.0	3.990
2.0	1.178
3.0	0.500
4.5	0.270
6.5	0.128
8.5	0.050

B14.7

Z (cm)	<C>(g/l)
1.0	4.965
2.0	1.453
3.0	0.624
4.5	0.297
6.5	0.136
8.5	0.057

B14.8

Z (cm)	<C>(g/l)
0.8	5.336
1.8	1.548
2.8	0.663
4.3	0.342
6.3	0.157
8.3	0.070

B14.9

Z (cm)	<C>(g/l)
0.5	8.677
1.5	2.587
2.5	0.988
4.0	0.459
6.0	0.194
8.0	0.093

Table 3.12 Measured vertical concentration distributions

BT14.10

Z (cm)	<C>(g/l)
0.7	4.454
1.7	1.402
2.7	0.811
4.2	0.275
6.2	0.128
8.2	0.048

B15.1

Z (cm)	<C>(g/l)
0.7	2.923
1.7	0.611
2.7	0.280
4.2	0.153
6.2	0.072
8.2	0.037

B15.2

Z (cm)	<C>(g/l)
0.7	3.990
1.7	0.705
2.7	0.332
4.2	0.167
6.2	0.072
8.2	0.035

Table 3.13 Measured vertical concentration distributions

B15.3

Z (cm)	<C>(g/l)
1.2	1.310
2.2	0.318
3.2	0.124
4.7	0.063
6.7	0.035
8.7	0.020

B15.4

Z (cm)	<C>(g/l)
1.2	1.137
2.2	0.309
3.2	0.126
4.7	0.072
6.7	0.041
8.7	0.026

B15.5

Z (cm)	<C>(g/l)
1.0	2.053
2.0	0.464
3.0	0.195
4.5	0.099
6.5	0.049
8.5	0.028

B15.6

Z (cm)	<C>(g/l)
1.2	1.253
2.2	0.335
3.2	0.156
4.7	0.086
6.7	0.049
8.7	0.030

B16.1

Z (cm)	<C>(g/l)
1.4	0.893
2.4	0.309
3.4	0.156
4.9	0.085
6.9	0.046
8.9	0.020

B16.2

Z (cm)	<C>(g/l)
0.5	6.496
1.5	1.178
2.5	0.468
4.0	0.212
6.0	0.104
8.0	0.052

Table 3.14 Measured vertical concentration distributions

B16.3

Z (cm)	<C>(g/l)
0.8	1.520
1.8	0.499
2.8	0.208
4.3	0.113
6.3	0.052
8.3	0.024

B16.4

Z (cm)	<C>(g/l)
1.5	0.696
2.5	0.284
3.5	0.143
5.0	0.077
7.0	0.029
9.0	0.017

B16.5

Z (cm)	<C>(g/l)
0.7	3.434
1.7	0.705
2.7	0.286
4.2	0.126
6.2	0.061
8.2	0.026

B16.6

Z (cm)	<C>(g/l)
0.9	2.181
1.9	0.593
2.9	0.247
4.4	0.126
6.4	0.058
8.4	0.026

B16.7

Z (cm)	<C>(g/l)
1.0	1.624
2.0	0.646
3.0	0.208
4.5	0.108
6.5	0.052
8.5	0.022

Table 3.15 Measured vertical concentration distributions

B17.1

Z (cm)	<C>(g/l)	Z (cm)	<C>(g/l)	Z (cm)	<C>(g/l)
2.3	0.522	2.1	0.510	1.9	0.673
3.3	0.284	3.1	0.249	2.9	0.318
4.3	0.150	4.1	0.111	3.9	0.150
5.8	0.054	5.6	0.050	5.4	0.038
7.8	0.015	7.6	0.017	7.4	0.017
9.8	0.004	9.6	0.006	9.4	0.006

B17.2

Z (cm)	<C>(g/l)	Z (cm)	<C>(g/l)	Z (cm)	<C>(g/l)
1.9	0.835	1.8	0.754	1.7	0.615
2.9	0.292	2.8	0.404	2.7	0.318
3.9	0.202	3.8	0.208	3.7	0.162
5.4	0.095	5.3	0.095	5.2	0.068
7.4	0.032	7.3	0.032	7.2	0.023
9.4	0.007	9.3	0.004	9.2	-

B17.3

Z (cm)	<C>(g/l)	Z (cm)	<C>(g/l)	Z (cm)	<C>(g/l)
1.7	1.009	1.9	0.510	2.1	0.986
2.7	0.646	2.9	0.267	3.1	0.533
3.7	0.215	3.9	0.137	4.1	0.299
5.2	0.081	5.4	0.063	5.6	0.131
7.2	0.017	7.4	0.017	7.6	0.037
9.2	0.004	9.4	-	9.6	0.007

B17.4

Z (cm)	<C>(g/l)	Z (cm)	<C>(g/l)	Z (cm)	<C>(g/l)
2.1	1.114	2.0	0.487	1.8	0.673
3.1	0.645	3.0	0.232	2.8	0.361
4.1	0.338	4.0	0.117	3.8	0.182
5.6	0.149	5.5	0.050	5.3	0.077
7.6	0.044	7.5	0.012	7.3	0.017
9.6	0.007	9.5	0.004	9.3	0.004

Table 3.16 Measured vertical concentration distributions

B17.5

Z (cm)	<C>(g/l)	Z (cm)	<C>(g/l)	Z (cm)	<C>(g/l)
1.8	0.824	2.0	0.684	2.2	0.568
2.8	0.421	3.0	0.292	3.2	0.301
3.8	0.208	4.0	0.150	4.2	0.169
5.3	0.094	5.5	0.076	5.7	0.081
7.3	0.044	7.5	0.034	7.7	0.023
9.3	0.009	9.5	0.004	9.7	0.004

B17.6

Z (cm)	<C>(g/l)	Z (cm)	<C>(g/l)	Z (cm)	<C>(g/l)
2.2	1.183	1.9	0.603	1.6	0.638
3.2	0.516	2.9	0.292	2.6	0.361
4.2	0.364	3.9	0.150	3.6	0.215
5.7	0.171	5.4	0.063	5.1	0.081
7.7	0.035	7.4	0.026	7.1	0.032
9.7	0.007	9.4	0.004	9.1	0.007

B17.7

Z (cm)	<C>(g/l)	Z (cm)	<C>(g/l)	Z (cm)	<C>(g/l)
1.6	0.626	1.8	0.754	1.9	0.661
2.6	0.344	2.8	0.327	2.9	0.258
3.6	0.176	3.8	0.156	3.9	0.104
5.1	0.072	5.3	0.072	5.4	0.050
7.1	0.026	7.3	0.023	7.4	0.015
9.1	0.006	9.3	0.009	9.4	0.006

B17.8

Z (cm)	<C>(g/l)	Z (cm)	<C>(g/l)	Z (cm)	<C>(g/l)
1.9	0.777	1.9	0.650	1.9	0.719
2.9	0.326	2.9	0.241	2.9	0.284
3.9	0.169	3.9	0.130	3.9	0.150
5.4	0.077	5.4	0.063	5.4	0.072
7.4	0.023	7.4	0.029	7.4	0.026
9.4	0.006	9.4	0.006	9.4	0.006

Table 3.17 Measured vertical concentration distributions

B17.9

Z (cm)	<C>(g/l)	Z (cm)	<C> (g/l)	Z (cm)	<C>(g/l)
1.9	0.545	1.9	0.429	1.8	0.835
2.9	0.301	2.9	0.241	2.8	0.456
3.9	0.163	3.9	0.143	3.8	0.234
5.4	0.059	5.4	0.059	5.3	0.086
7.4	0.020	7.4	0.026	7.3	0.020
9.4	0.004	9.4	0.004	9.3	0.007

B17.10

Z (cm)	<C>(g/l)	Z (cm)	<C>(g/l)	Z (cm)	<C>(g/l)
1.8	0.650	1.9	0.580	1.9	0.406
2.8	0.387	2.9	0.292	2.9	0.224
3.8	0.208	3.9	0.156	3.9	0.117
5.3	0.068	5.4	0.081	5.4	0.045
7.3	0.012	7.4	0.038	7.4	0.017
9.3	0.004	9.4	0.011	9.4	0.002

B18.1

Z (cm)	<C>(g/l)	Z (cm)	<C>(g/l)	Z (cm)	<C>(g/l)
0.9	0.824	0.6	2.042	0.2	2.668
1.9	0.249	1.6	0.378	1.2	1.006
2.9	0.098	2.6	0.124	2.2	0.409
4.4	0.041	4.1	0.054	3.7	0.148
6.4	0.009	6.1	0.017	5.7	0.029
8.4	0.006	8.1	0.007	7.7	0.013

Table 3.18 Measured vertical concentration distributions

B18.2

Z (cm)	<C>(g/l)	Z (cm)	<C>(g/l)	Z (cm)	<C>(g/l)
0.7	0.626	0.3	3.737	0.0	9.048
1.7	0.275	1.3	0.628	1.0	1.221
2.7	0.117	2.3	0.319	2.0	0.377
4.2	0.054	3.8	0.144	3.5	0.135
6.2	0.023	5.8	0.046	5.5	0.040
8.2	0.011	7.8	0.014	7.5	0.007

B18.3

Z (cm)	<C>(g/l)	Z (cm)	<C>(g/l)	Z (cm)	<C>(g/l)
0.3	1.610	0.1	2.668	0.4	1.369
1.3	0.360	1.1	0.834	1.4	0.516
2.3	0.142	2.1	0.299	2.4	0.215
3.8	0.063	3.6	0.108	3.9	0.086
5.8	0.032	5.6	0.035	5.9	0.041
7.8	0.004	7.6	0.007	7.9	0.011

B18.4

Z (cm)	<C>(g/l)	Z (cm)	<C>(g/l)	Z (cm)	<C>(g/l)
0.7	3.404	0.1	7.331	0.2	2.571
1.7	0.748	1.1	1.299	1.2	1.531
2.7	0.377	2.1	0.449	2.2	0.650
4.2	0.198	3.6	0.207	3.7	0.112
6.2	0.052	5.6	0.099	5.7	0.020
8.2	0.018	7.6	0.017	7.7	0.011

B18.5

Z (cm)	<C>(g/l)	Z (cm)	<C>(g/l)	Z (cm)	<C>(g/l)
0.2	3.589	1.5	0.754	2.4	0.232
1.2	1.032	2.5	0.275	3.4	0.154
2.2	0.416	3.5	0.117	4.4	0.091
3.7	0.144	5.0	0.063	5.9	0.036
5.7	0.029	7.0	0.026	7.9	0.029
7.7	0.011	9.0	0.006	9.9	0.004

Table 3.19 Measured vertical concentration distributions

B19.1

Z (cm)	<C>(g/l)	Z (cm)	<C>(g/l)	Z (cm)	<C>(g/l)
0.3	4.120	0.2	20.000	0.5	10.900
1.3	1.360	1.2	3.400	1.5	3.250
2.3	0.561	2.2	1.270	2.5	1.470
3.8	0.213	3.7	0.553	4.0	0.661
5.8	0.046	5.7	0.165	6.0	0.206
7.8	0.011	7.7	0.033	8.0	0.030

B19.2

Z (cm)	<C>(g/l)	Z (cm)	<C>(g/l)	Z (cm)	<C>(g/l)
1.2	3.240	0.9	4.180	1.1	0.986
2.2	1.080	1.9	1.030	2.1	0.371
3.2	0.457	2.9	0.437	3.1	0.176
4.7	0.154	4.4	0.154	4.6	0.054
6.7	0.044	6.4	0.035	6.6	0.009
8.7	0.007	8.4	0.011	8.6	0.004

B19.3

Z (cm)	<C>(g/l)	Z (cm)	<C>(g/l)
1.5	0.580	1.7	0.557
2.5	0.216	2.7	0.190
3.5	0.085	3.7	0.085
5.0	0.032	5.2	0.028
7.0	0.029	7.2	0.017
9.0	0.004	9.2	0.004

Table 3.20 Measured vertical concentration distributions

B19.4

Z (cm)	<C>(g/l)	Z (cm)	<C>(g/l)	Z (cm)	<C>(g/l)
1.5	1.790	1.6	0.522	1.2	2.780
2.5	0.751	2.6	0.242	2.2	0.768
3.5	0.326	3.6	0.111	3.2	0.281
5.0	0.122	5.1	0.041	4.7	0.054
7.0	0.026	7.1	0.026	6.7	0.012
9.0	0.004	9.1	0.004	8.7	0.004

B19.5

Z (cm)	<C>(g/l)	Z (cm)	<C>(g/l)	Z (cm)	<C>(g/l)
1.4	0.522	1.3	1.990	1.7	2.780
2.4	0.190	2.3	0.820	2.7	1.000
3.4	0.078	3.3	0.373	3.7	0.373
4.9	0.045	4.8	0.140	5.2	0.140
6.9	0.023	6.8	0.029	7.2	0.044
8.9	0.006	8.8	0.004	9.2	0.007

B20.1

Z (cm)	<C>(g/l)	Z (cm)	<C>(g/l)
1.6	0.371	1.9	0.220
2.6	0.112	2.9	0.112
3.6	0.052	3.9	0.039
5.1	0.023	5.4	0.018
7.1	0.017	7.4	0.012
9.1	0.002	9.4	0.004

B20.2

Z (cm)	<C>(g/l)	Z (cm)	<C>(g/l)
0.9	0.267	0.2	1.580
1.9	0.095	1.2	0.285
2.9	0.046	2.2	0.111
4.4	0.045	3.7	0.073
6.4	0.011	5.7	0.026
8.4	0.004	7.7	0.007

Table 3.21 Measured vertical concentration distributions

B20.3

Z (cm)	<C>(g/l)	Z (cm)	<C>(g/l)
0.2	3.600	0.0	5.150
1.2	0.561	1.0	0.431
2.2	0.176	2.0	0.144
3.7	0.064	3.5	0.064
5.7	0.035	5.5	0.032
7.7	0.007	7.5	0.011

B20.4

Z (cm)	<C>(g/l)	Z (cm)	<C>(g/l)
0.4	1.790	0.4	1.170
1.4	0.319	1.4	0.224
2.4	0.117	2.4	0.046
3.9	0.045	3.9	0.036
5.9	0.020	5.9	0.012
7.9	0.011	7.9	0.004

B20.5

Z (cm)	<C>(g/l)	Z (cm)	<C>(g/l)
0.6	1.320	0.8	0.905
1.6	0.276	1.8	0.267
2.6	0.104	2.8	0.091
4.1	0.032	4.3	0.054
6.1	0.012	6.3	0.029
8.1	0.004	8.3	0.011

Table 3.22 Measured vertical concentration distributions

experiment no.	C_o (g/l)	C (at 1 cm) (g/l)	C (at 10 cm) (g/l)	α
1	15-20	2.5	0.020	2.1
2	13	0.7	0.006	2.1
3	4-6	1.0	0.010	2.0
4	8-12	3.5	0.030	2.1
5	3-4	0.6	0.006	2.0
6	6-7	2.0	0.020	2.0
7	10-14	3.0	0.027	2.0
8	12-20	4.1	0.042	2.0
9	30-50	19.0	0.095	2.3
10	7-11	2.7	0.029	2.0
11	20-40	5.1	0.044	2.1
12	100-200	73.0	0.500	2.2
13	11-20	3.1	0.023	2.0
14	11-15	5.0	0.050	2.0
15	10-15	1.7	0.021	1.9
16	14-20	1.8	0.020	2.0
				2.1 ± 0.1 (5%)

Table 3.23 Concentration profile characteristics - plane bed regime

exp. #	C_o (g/l)	r_c (cm)
17	2.5	1.6
18	4.2-6.5	0.7-0.8
19	4.5-6.0	1.1-1.3
20	0.9-1.2	1.0-1.2

Table 3.24 Concentration profile characteristics - rippled-bed regime

Experiment no.	η (cm)	λ (cm)	speed (cm/min)	2D/3D/plane
1	-	-	-	plane
2	0.4	8.7	3.0	2D
3	-	-	-	plane
4	-	-	-	plane
5	0.3	8.4	3.0	2D
6	-	-	-	plane
7	-	-	-	plane
8	-	-		
9	-	-		
10	-	-		
11	-	-		
12	-	-		
13	-	-		
14	-	-		
15	-	-		
16	-	-		
17	1.4	11.0	0.6	3D
18	0.9	9.0	1.2	3D
19	1.1	9.8	0.9	3D
20	0.7	9.1	1.6	2D

Table 3.25 Measured ripple characteristics

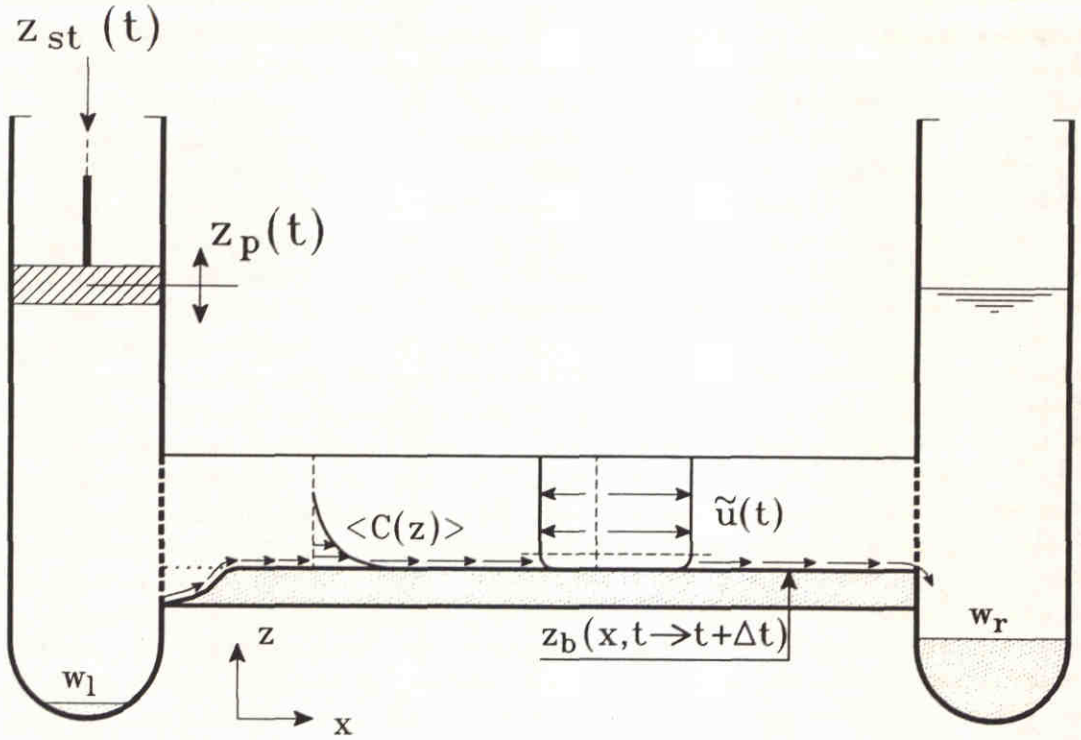

Imposed : – steer signal piston motion

Measured : – piston motion

– water velocity $\tilde{u}(t)$ (outside boundary layer)

– time-averaged concentration distribution $\langle C(z) \rangle$

– net (time-averaged) sediment transport rate $\langle q_s(x) \rangle$ (mass conservation technique)

IMPOSED/MEASURED PARAMETERS		
DELFT HYDRAULICS	H 840	FIG. 2.1

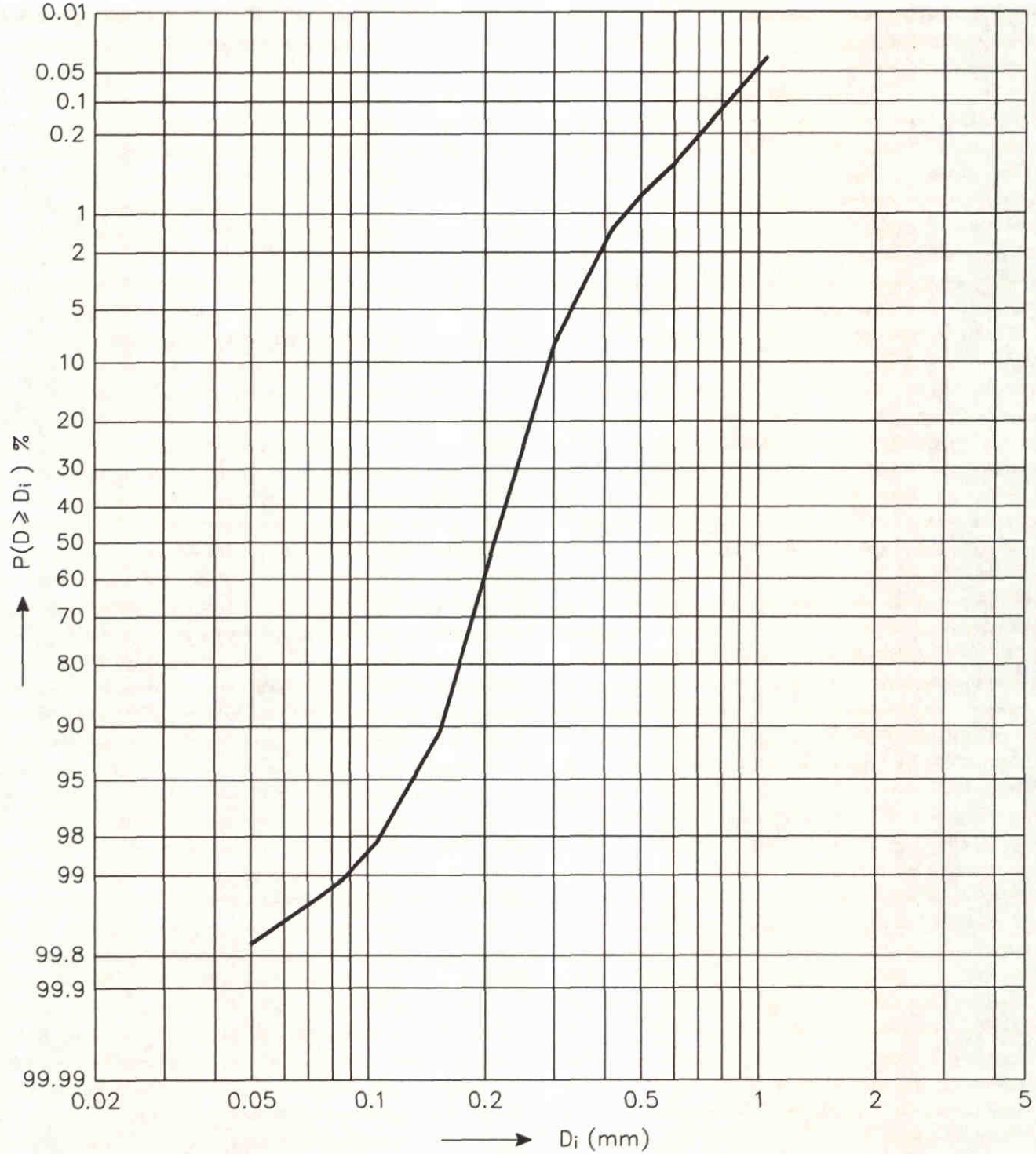

GRAIN–SIZE DISTRIBUTION

DELFT HYDRAULICS | H 840 | FIG. 2.2

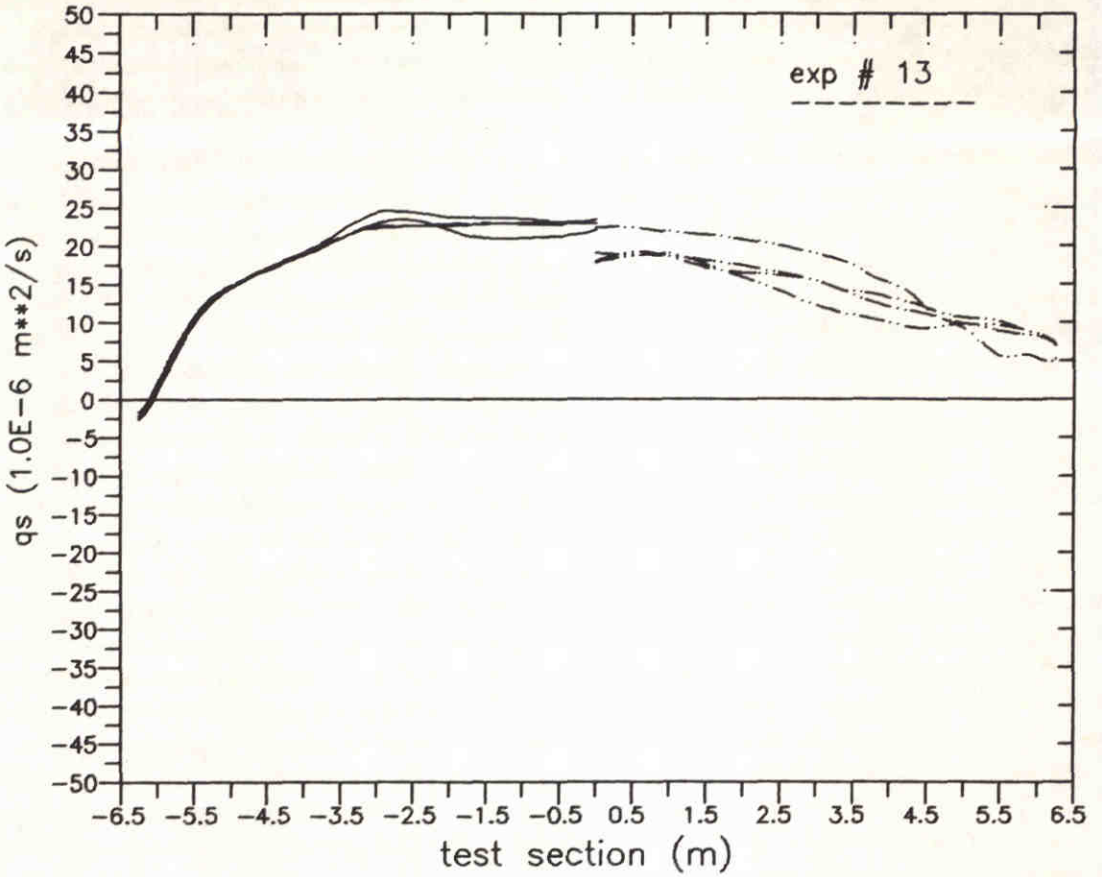

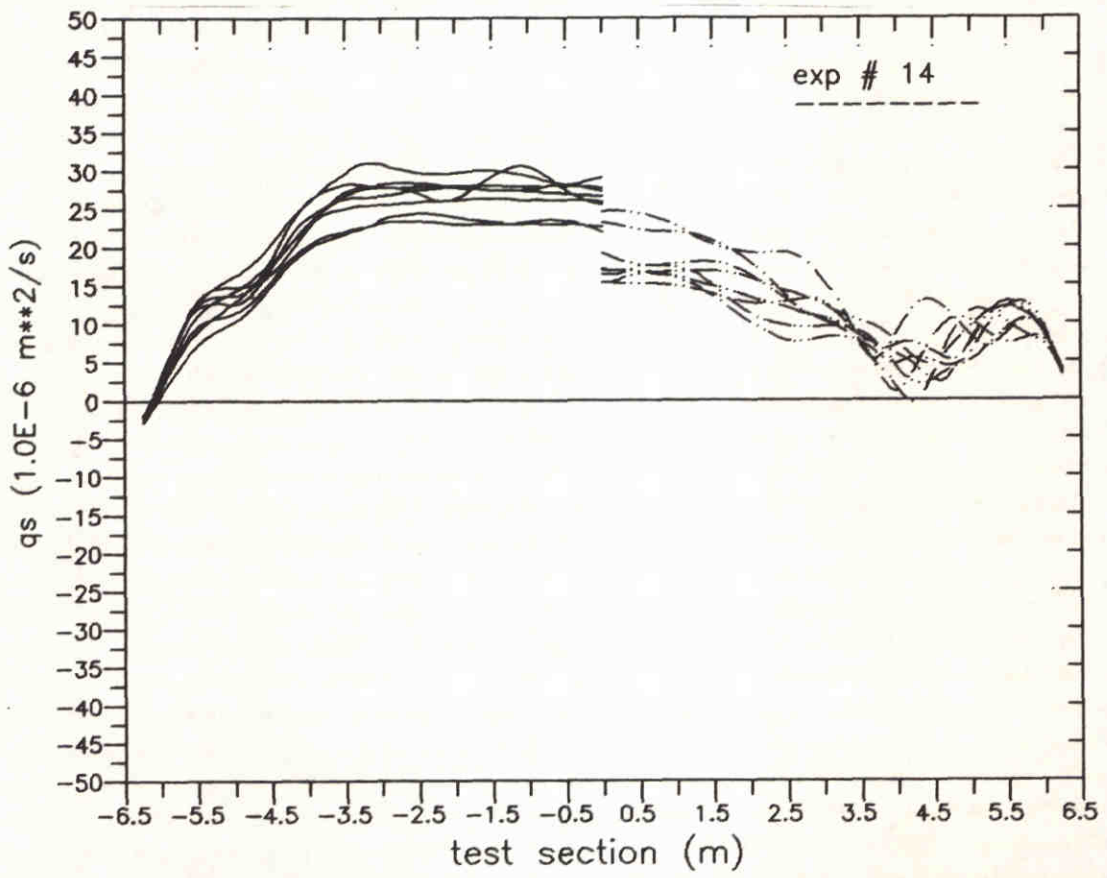

MEASURED SEDIMENT TRANSPORT RATES
ALONG THE TUNNEL TEST SECTION

DELFT HYDRAULICS | H 840 | FIG. 3.1

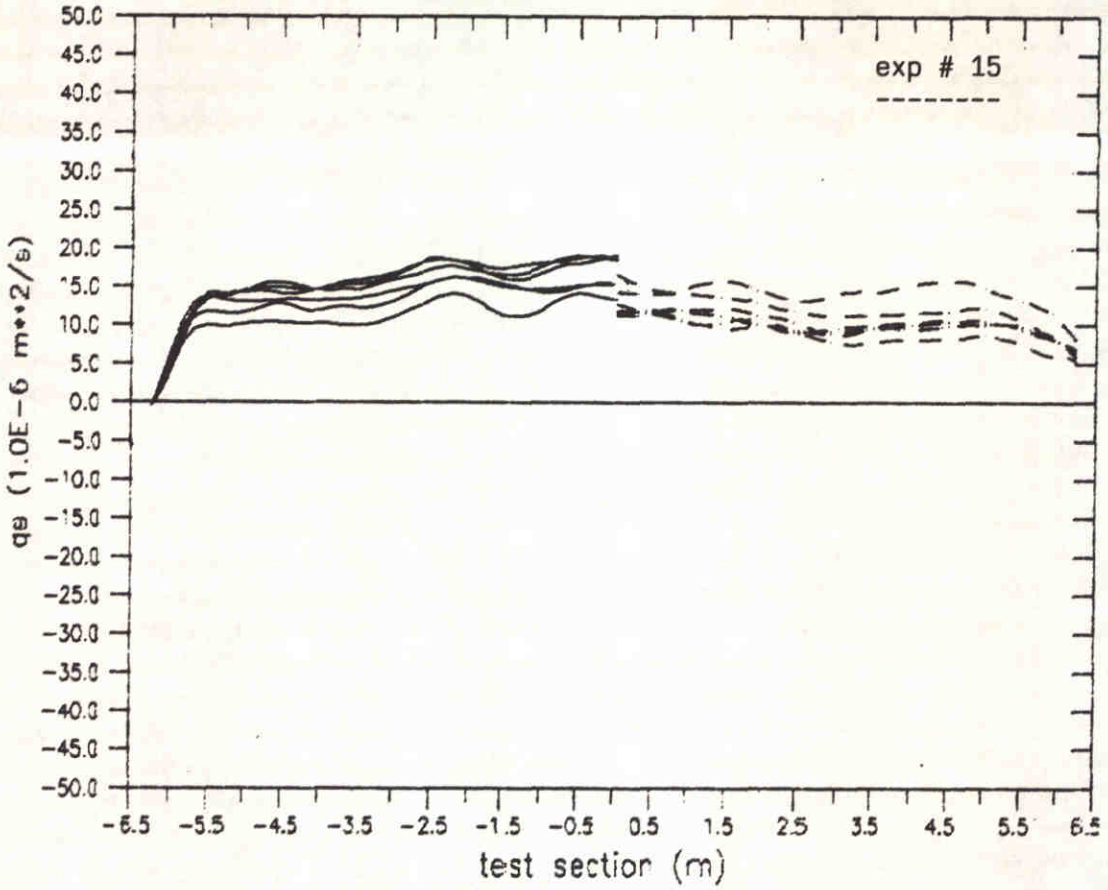

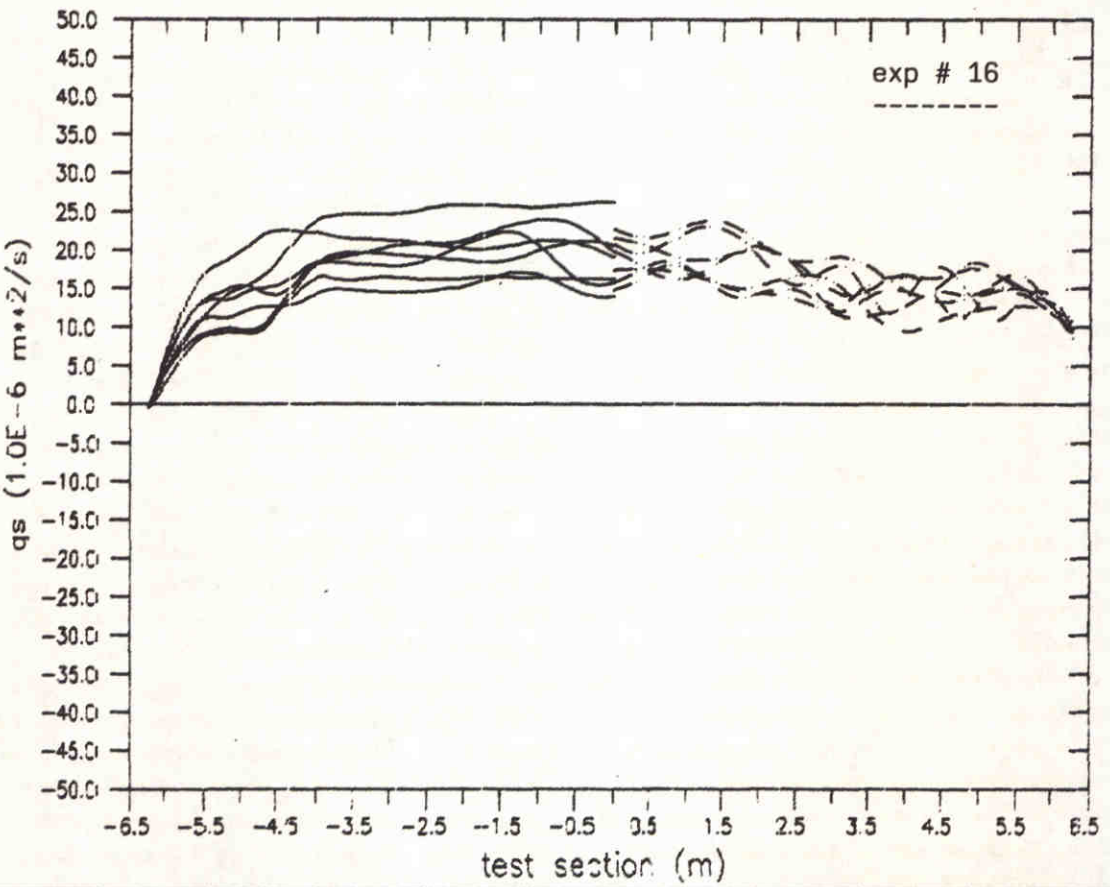

MEASURED SEDIMENT TRANSPORT RATES
ALONG THE TUNNEL TEST SECTION

DELFT HYDRAULICS | H 840 | FIG. 3.2

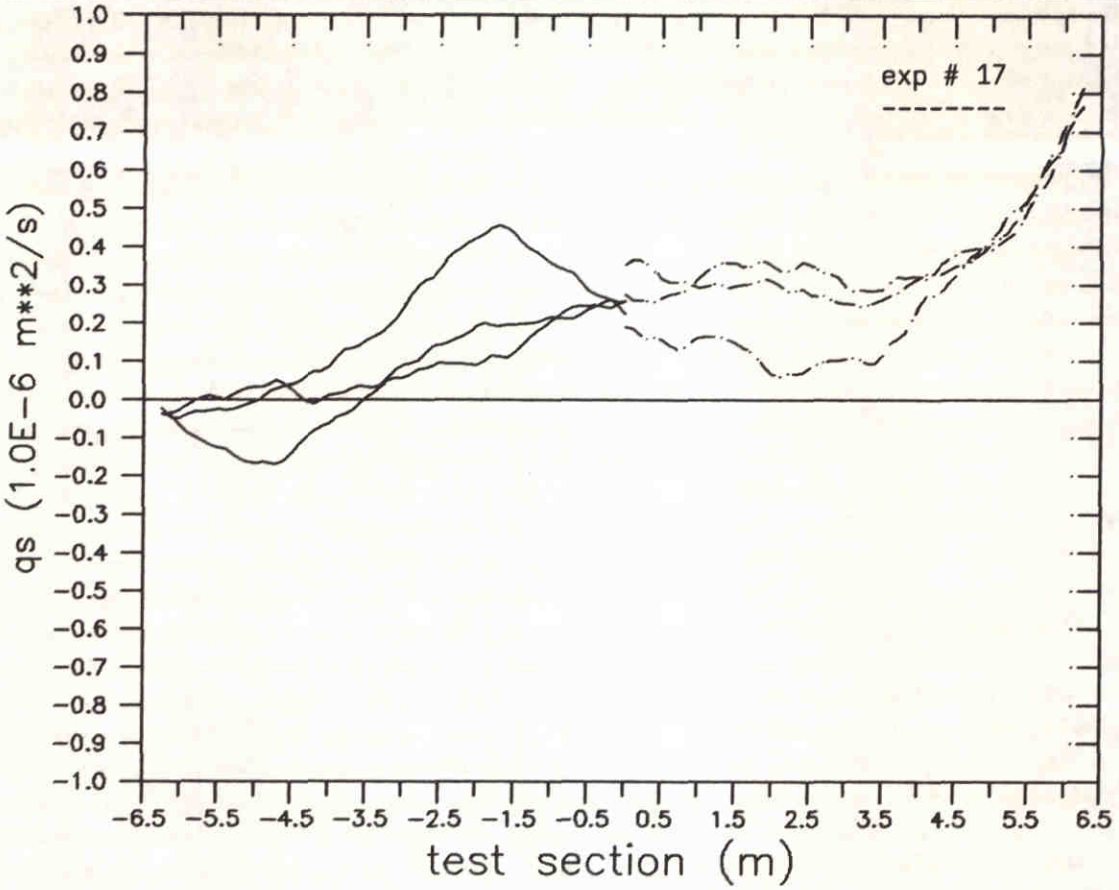

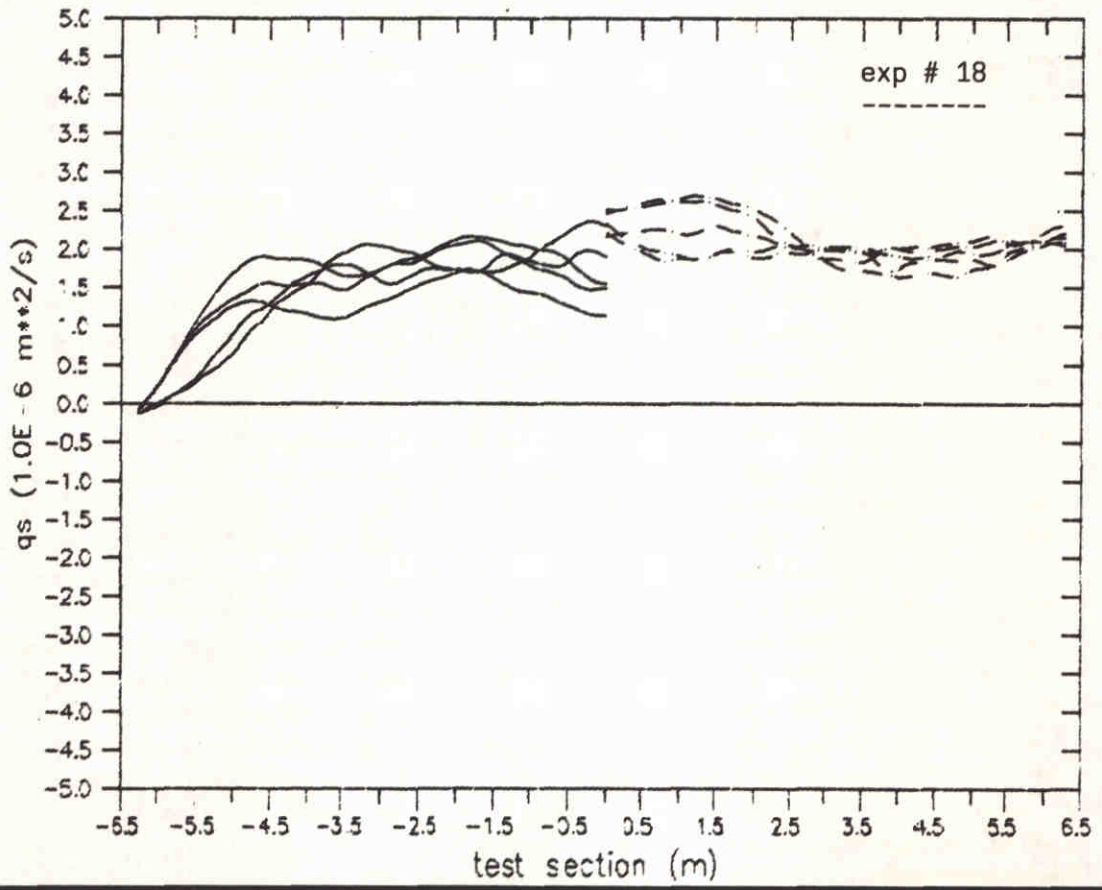

MEASURED SEDIMENT TRANSPORT RATES
ALONG THE TUNNEL TEST SECTION

DELFT HYDRAULICS | H 840 | FIG. 3.3

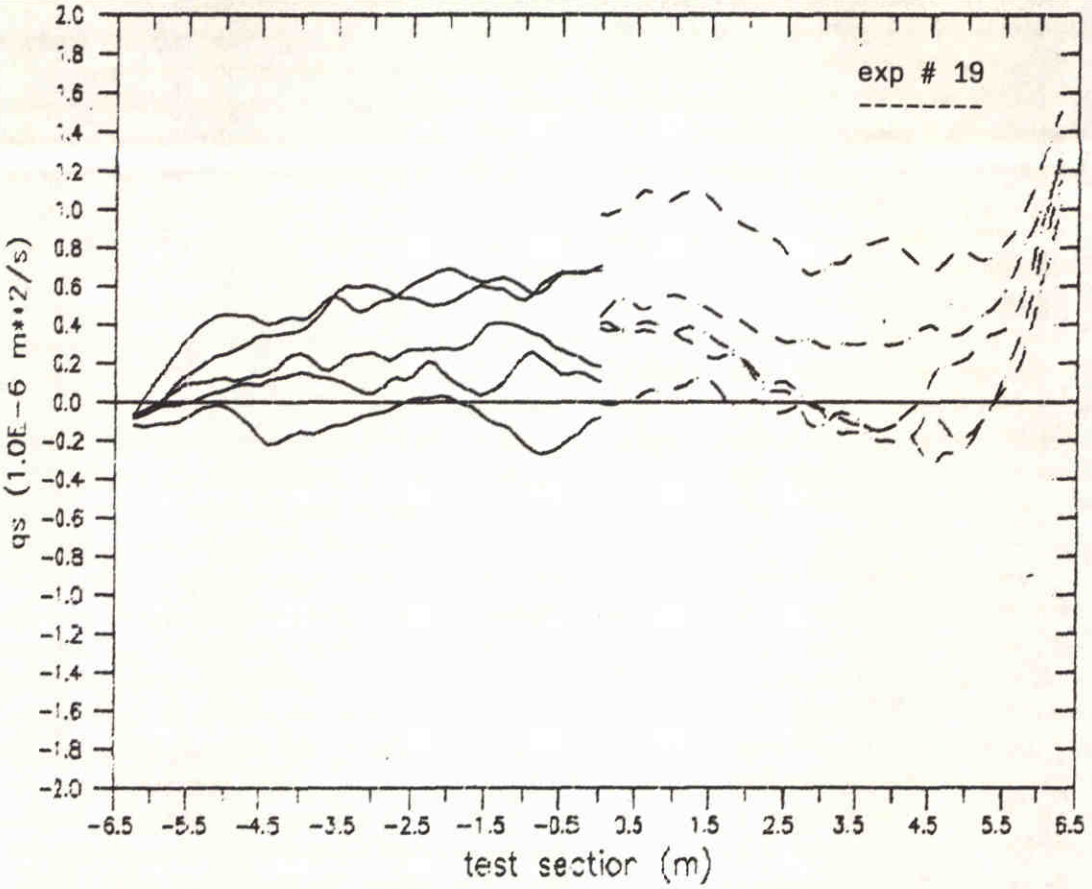

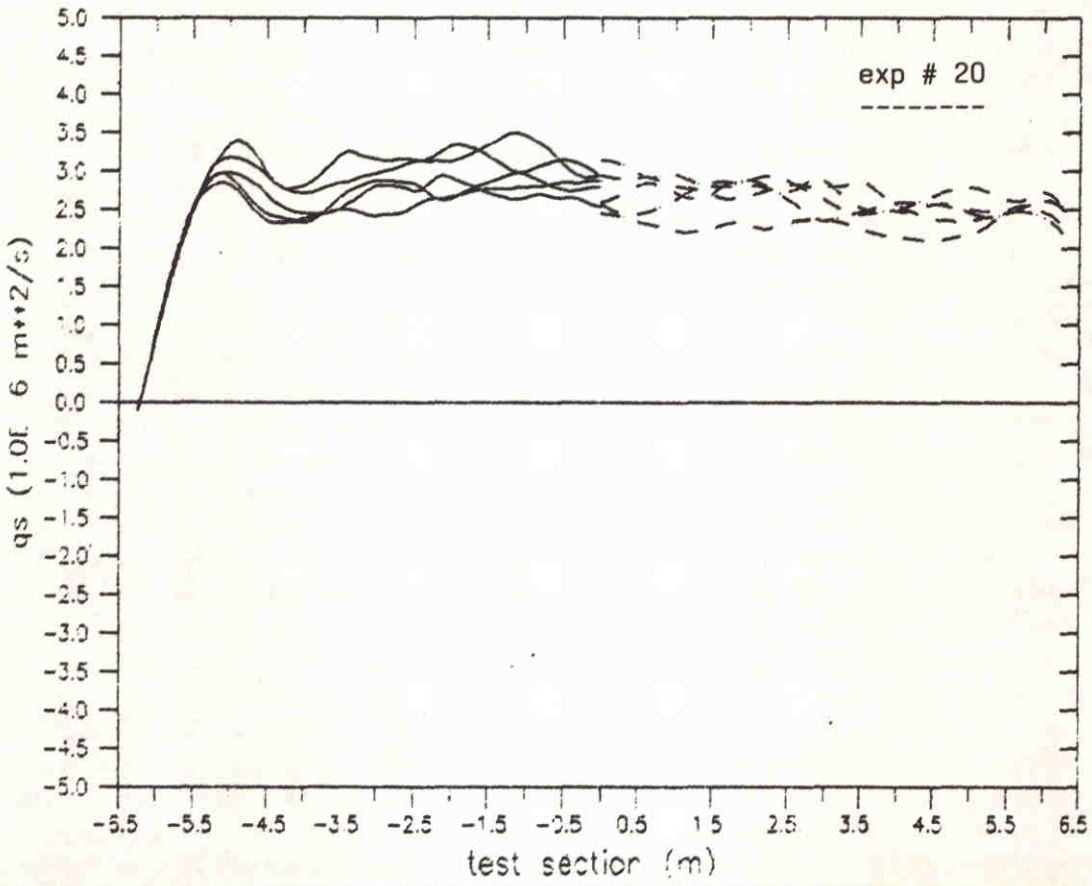

MEASURED SEDIMENT TRANSPORT RATES
ALONG THE TUNNEL TEST SECTION

DELFT HYDRAULICS | H 840 | FIG. 3.4

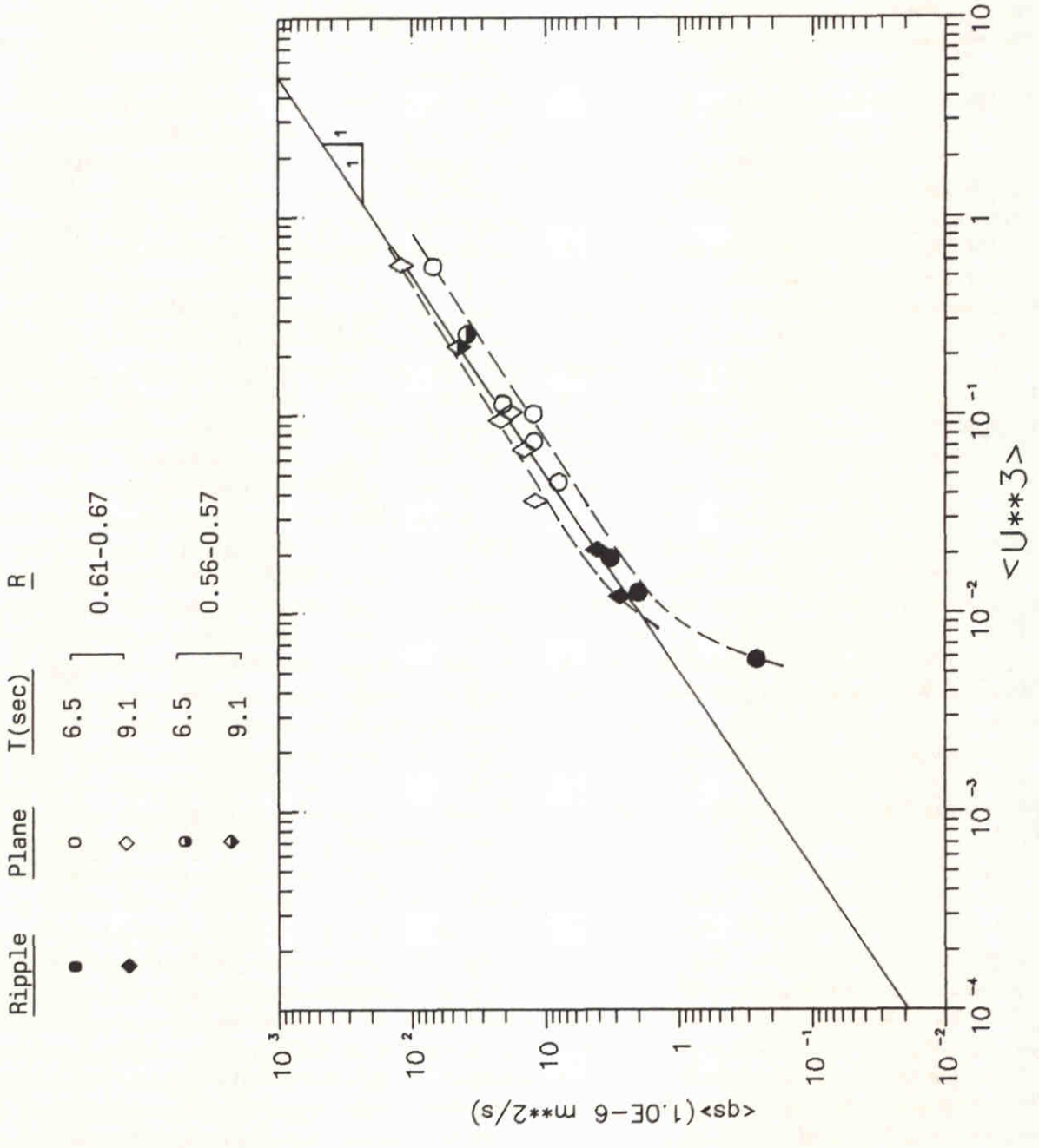

MEASURED SEDIMENT TRANSPORT RATES AS A FUNCTION OF VELOCITY MOMENTS $\langle U^3 \rangle$

DELFT HYDRAULICS | H 840 | FIG. 3.5

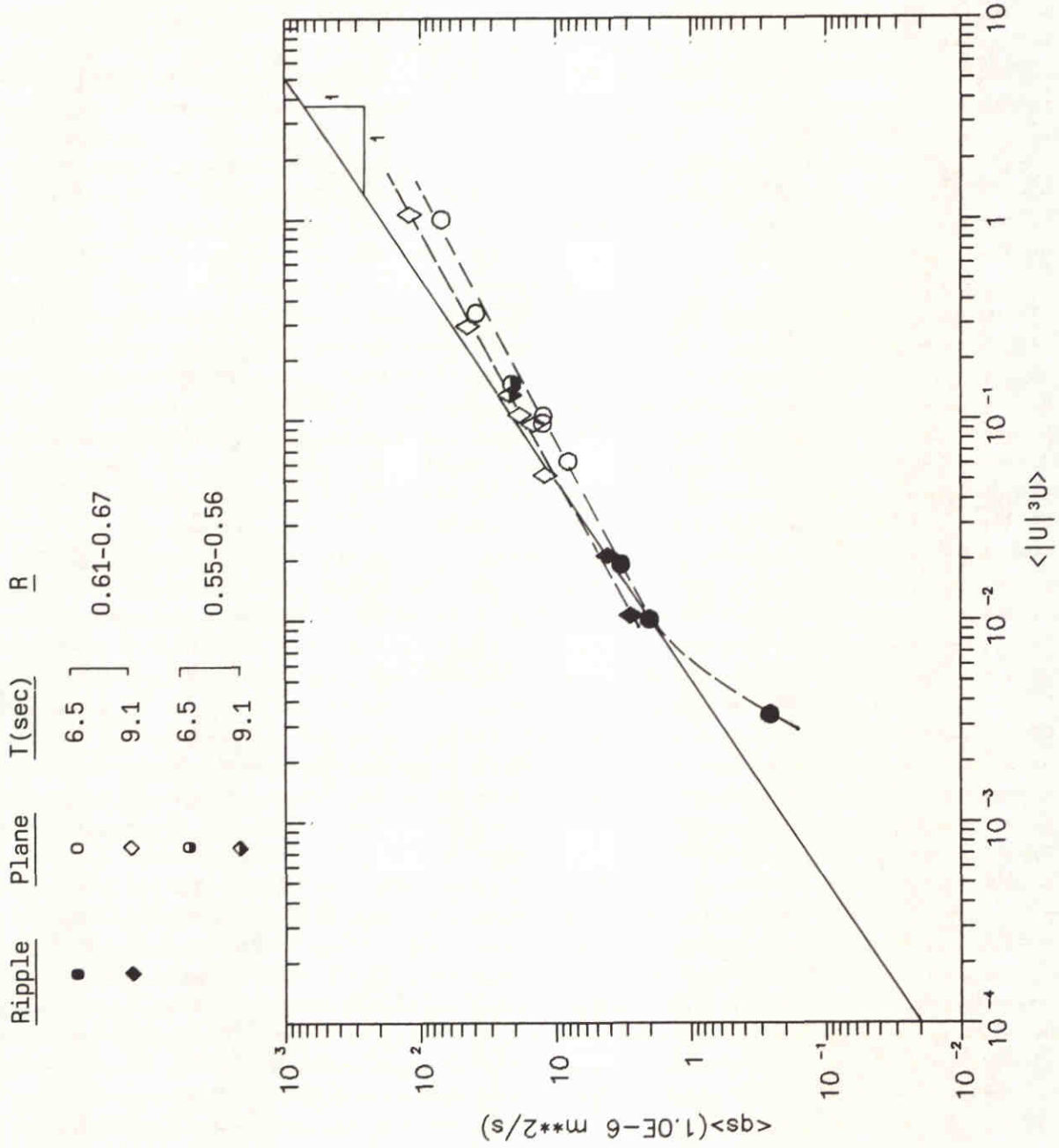

MEASURED SEDIMENT TRANSPORT RATES AS A FUNCTION OF VELOCITY MOMENTS $\langle |U^3|U \rangle$

DELFT HYDRAULICS | H 840 | FIG. 3.6

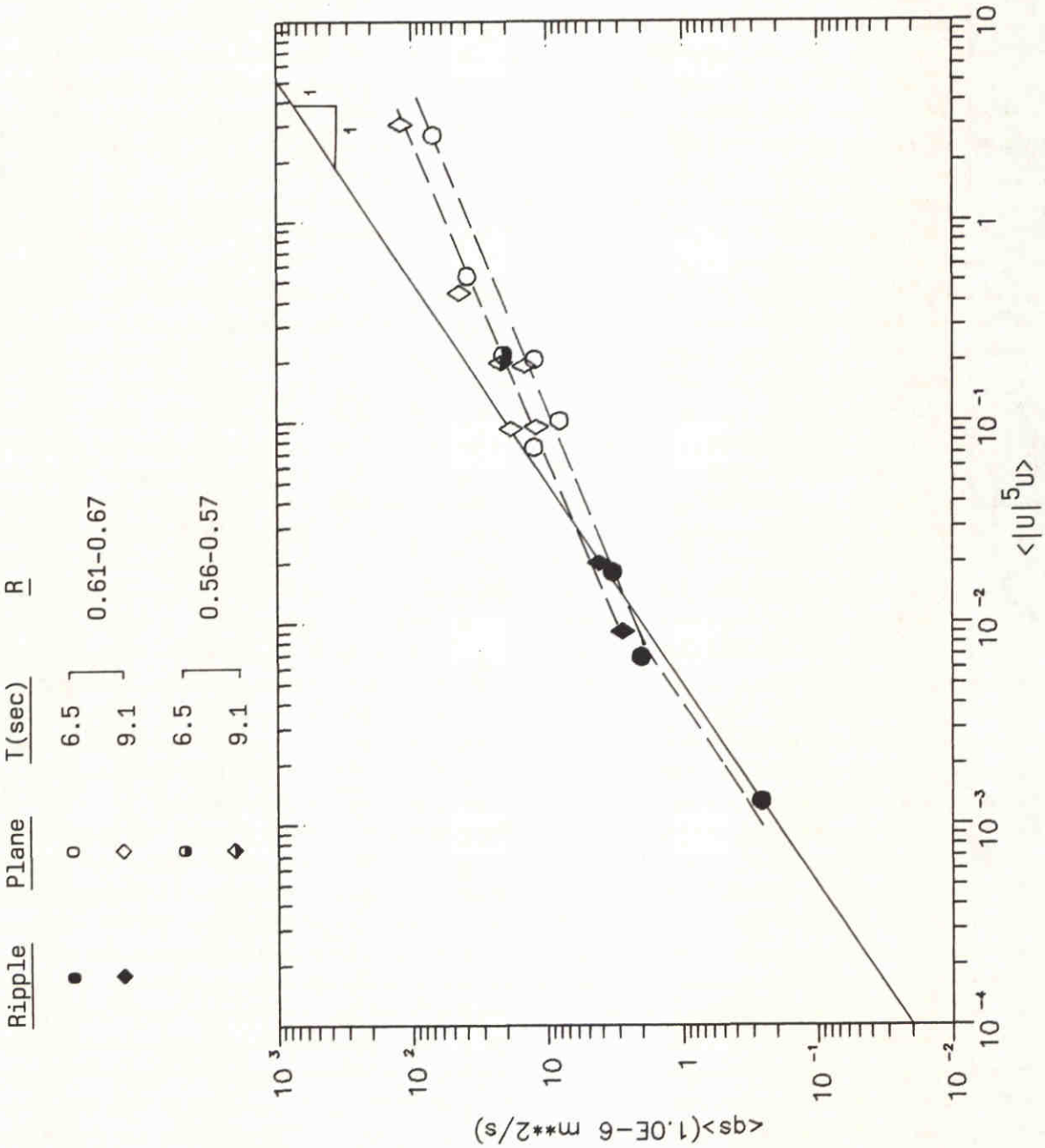

MEASURED SEDIMENT TRANSPORT RATES AS A FUNCTION OF VELOCITY MOMENTS $\langle |U^5|U \rangle$

DELFT HYDRAULICS | H 840 | FIG. 3.7

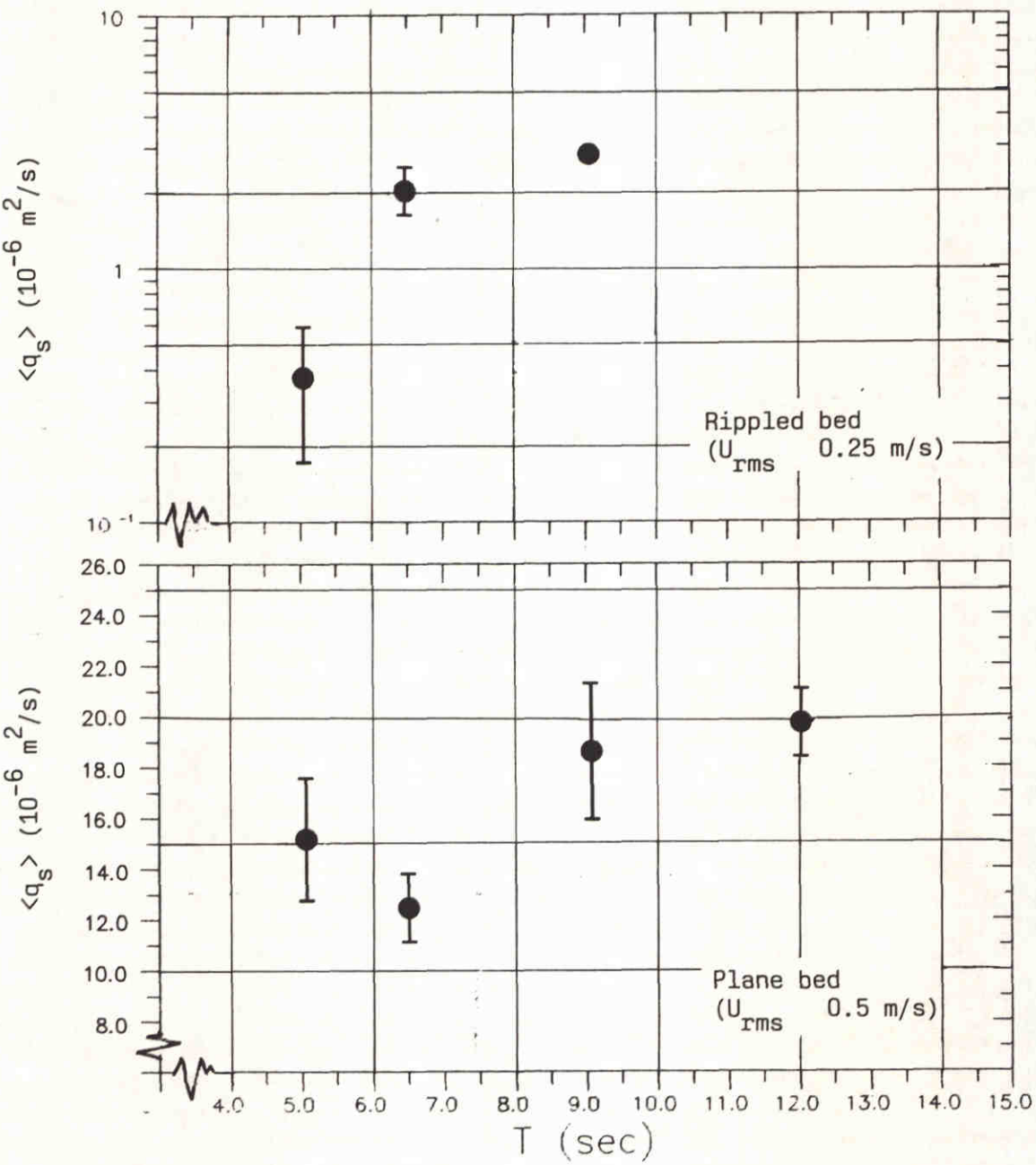

MEASURED NET TRANSPORT RATE – PERIOD INFLUENCE

DELFT HYDRAULICS | H 840 | FIG. 3.8

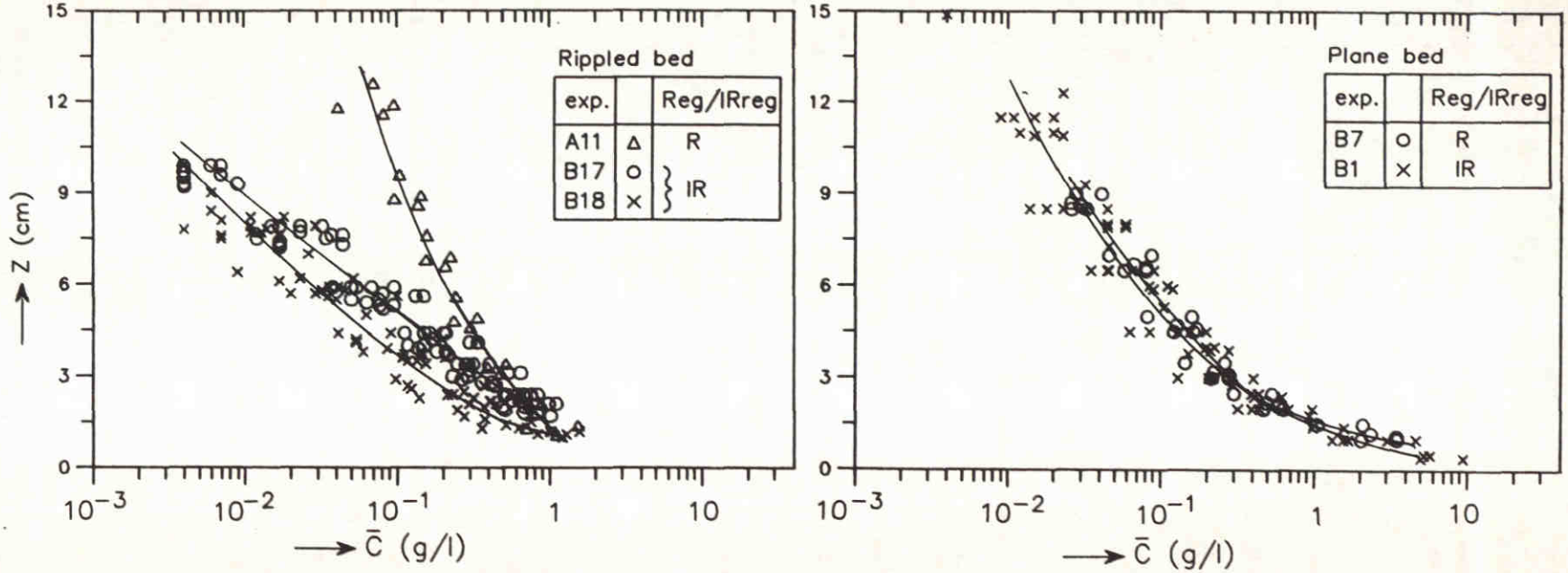

irregularity influence

(U_{rms}, $T \approx$ constant)

MEASURED TIME-AVERAGED CONCENTRATION PROFILES – IRREGULARITY INFLUENCE

DELFT HYDRAULICS

H 840

FIG. 3.9

MEASURED TIME-AVERAGED CONCENTRATION PROFILES - VELOCITY INFLUENCE

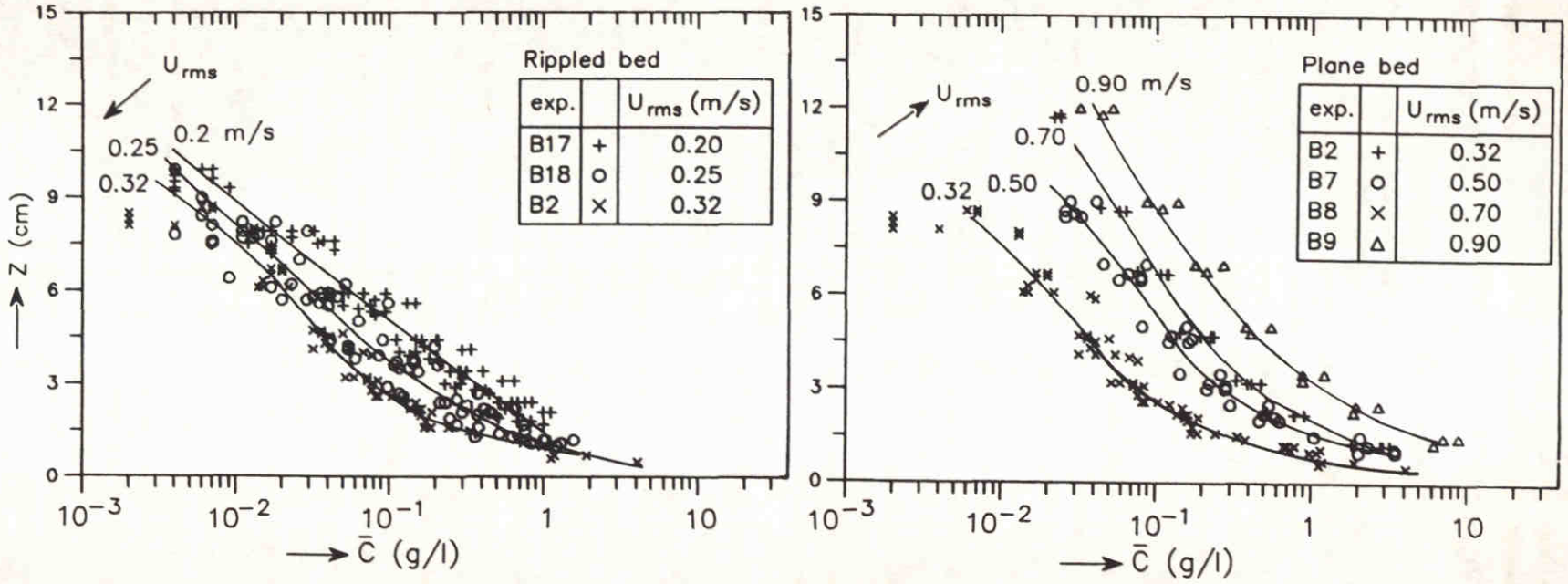

velocity influence (U_{rms})

(R,T constant)

DELFT HYDRAULICS

H 840

FIG. 3.10

MEASURED TIME-AVERAGED CONCENTRATION PROFILES - PERIOD INFLUENCE

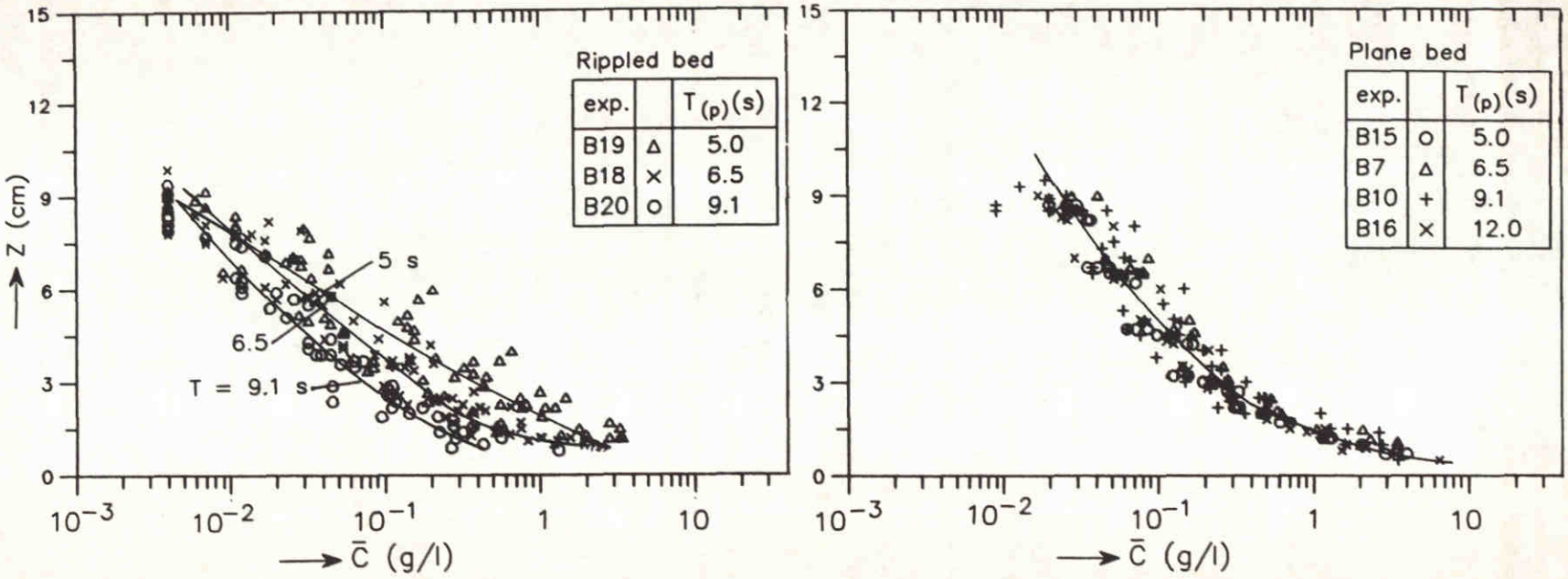

period influence

(U_{rms}, R constant)

DELFT HYDRAULICS

H 840

FIG. 3.11

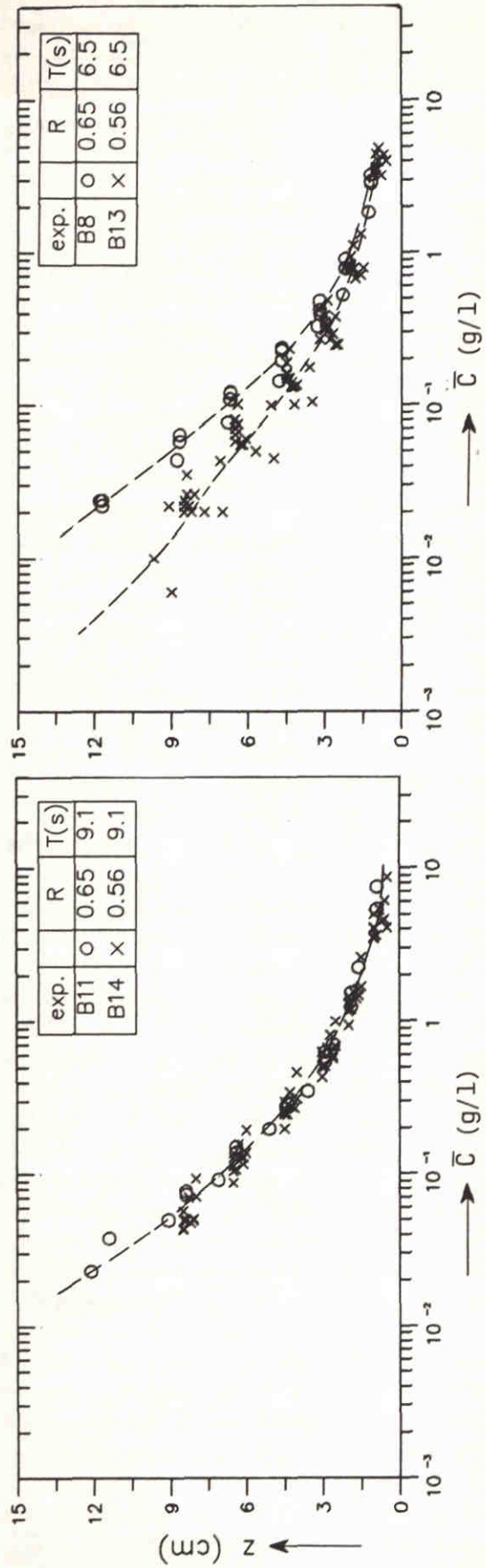

influence degree of asymmetry R
(U_{rms}, T constant)

MEASURED TIME-AVERAGED CONCENTRATION PROFILES – DEGREE OF ASYMMETRY INFLUENCE

DELFT HYDRAULICS | H 840 | FIG. 3.12

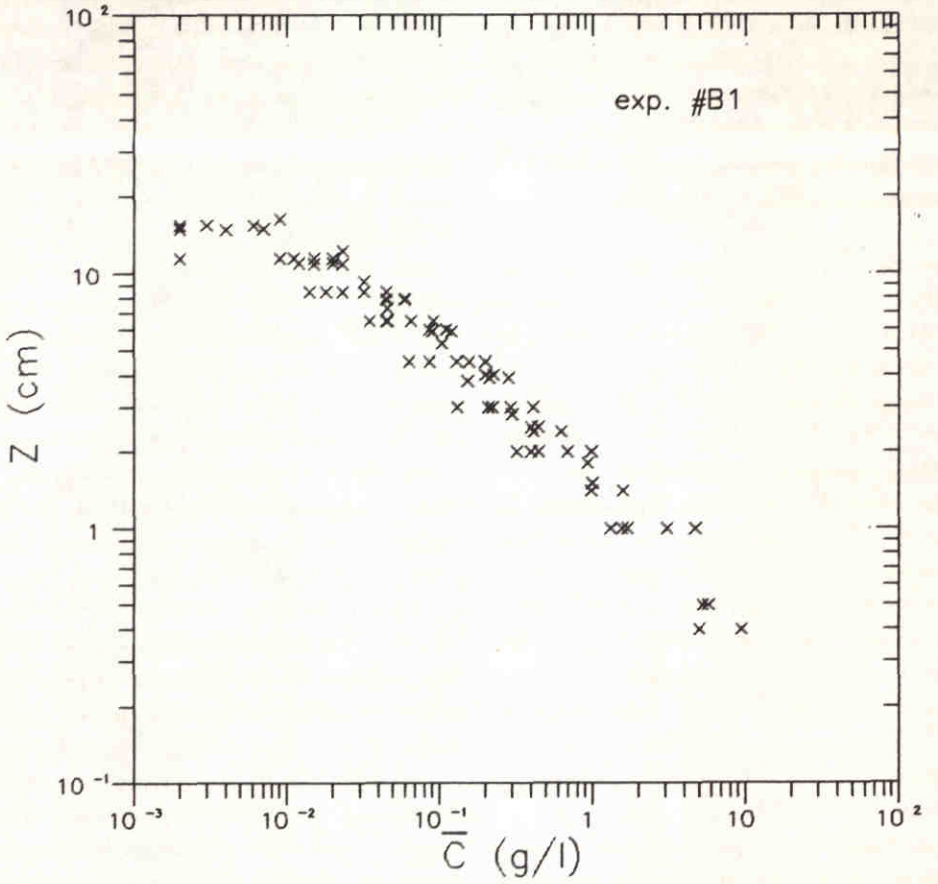

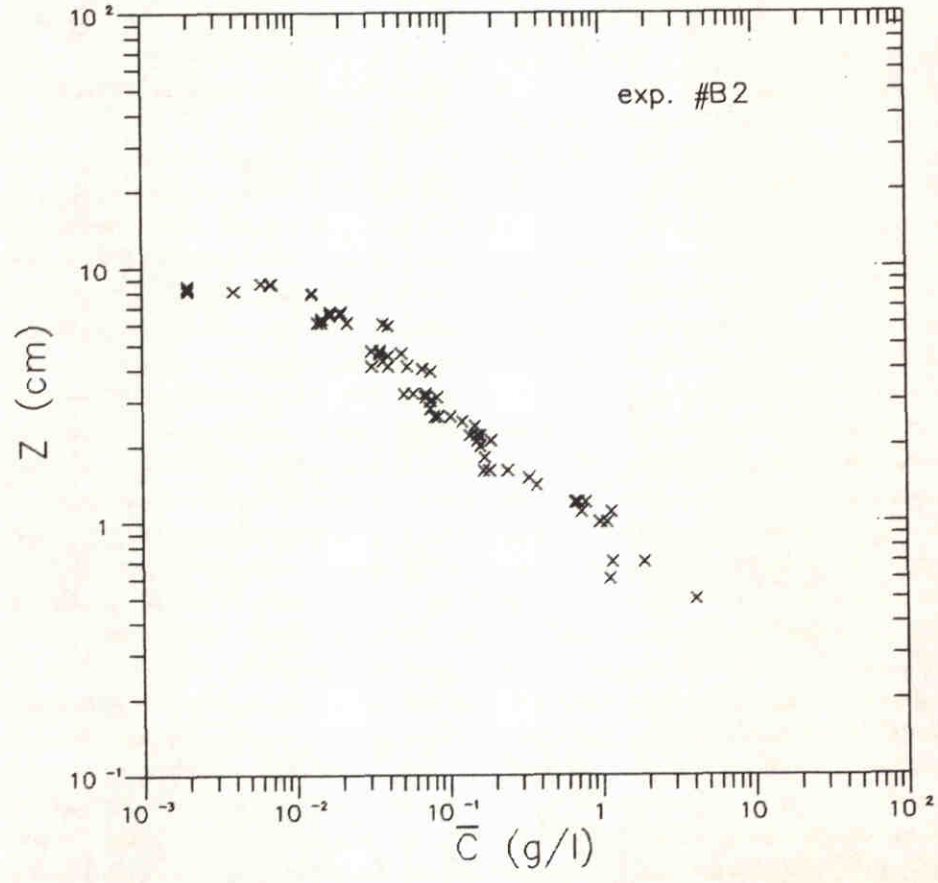

MEASURED TIME-AVERAGED CONCENTRATION PROFILES (LOG-LOG X-Y SCALES)

DELFT HYDRAULICS | H 840 | FIG. 3.13

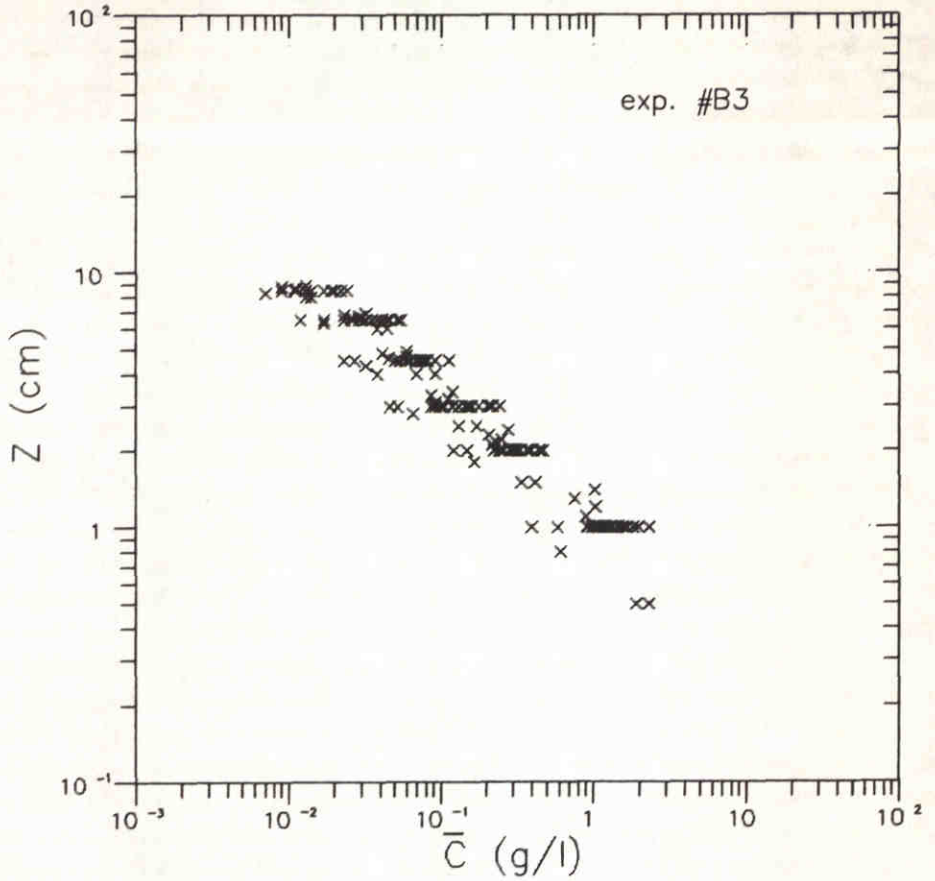

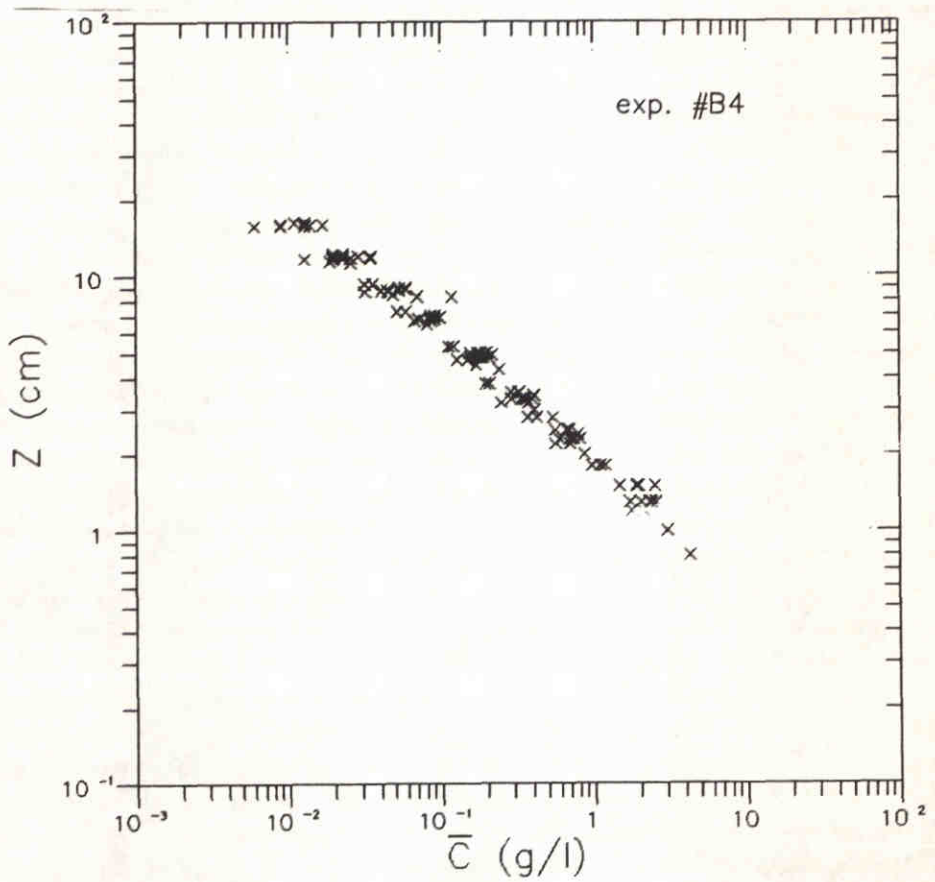

MEASURED TIME-AVERAGED CONCENTRATION PROFILES (LOG-LOG X-Y SCALES)

DELFT HYDRAULICS | H 840 | FIG. 3.14

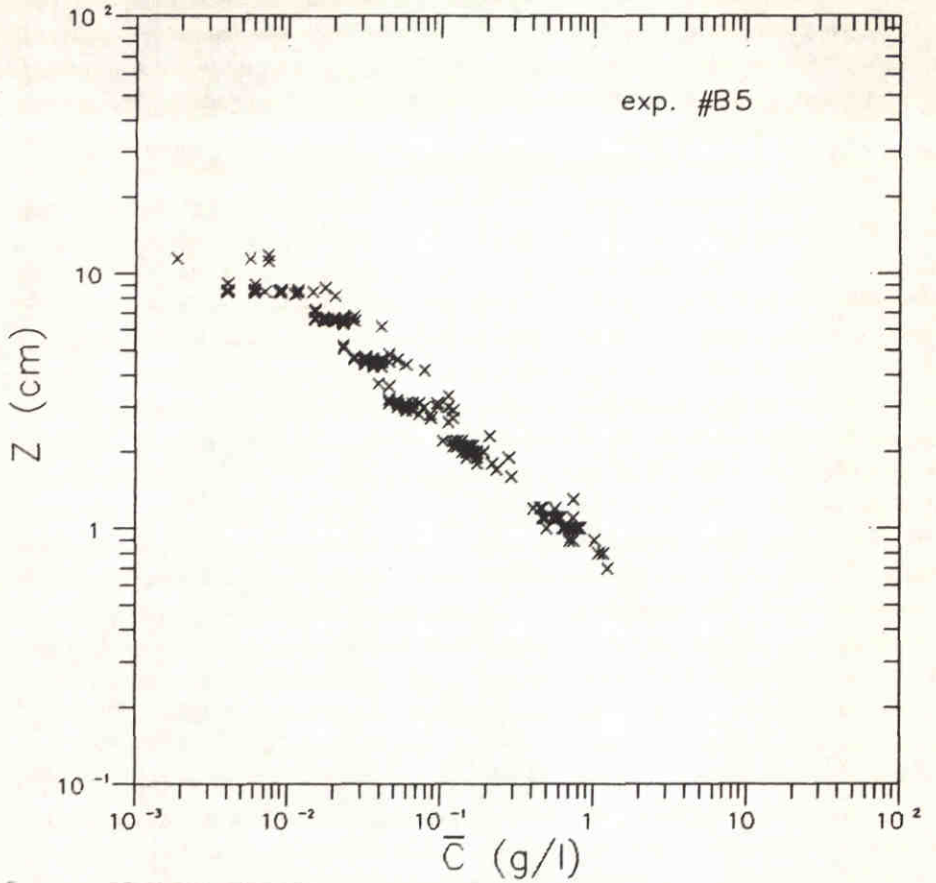

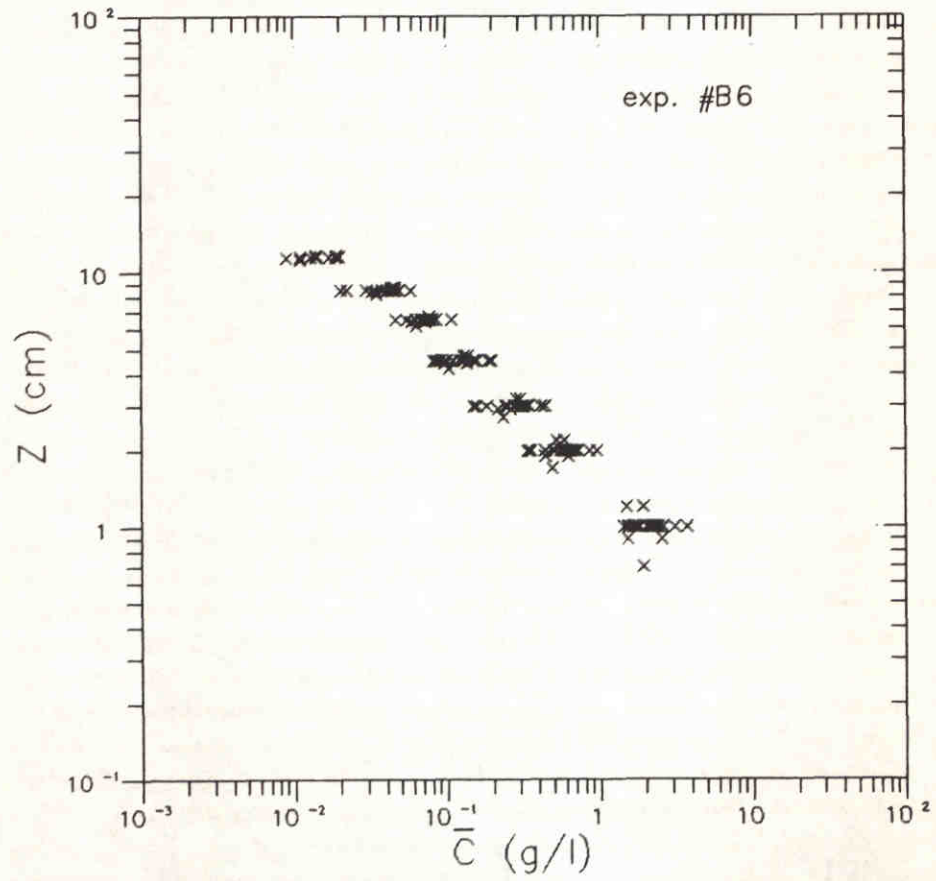

MEASURED TIME-AVERAGED CONCENTRATION PROFILES (LOG-LOG X-Y SCALES)

DELFT HYDRAULICS | H 840 | FIG. 3.15

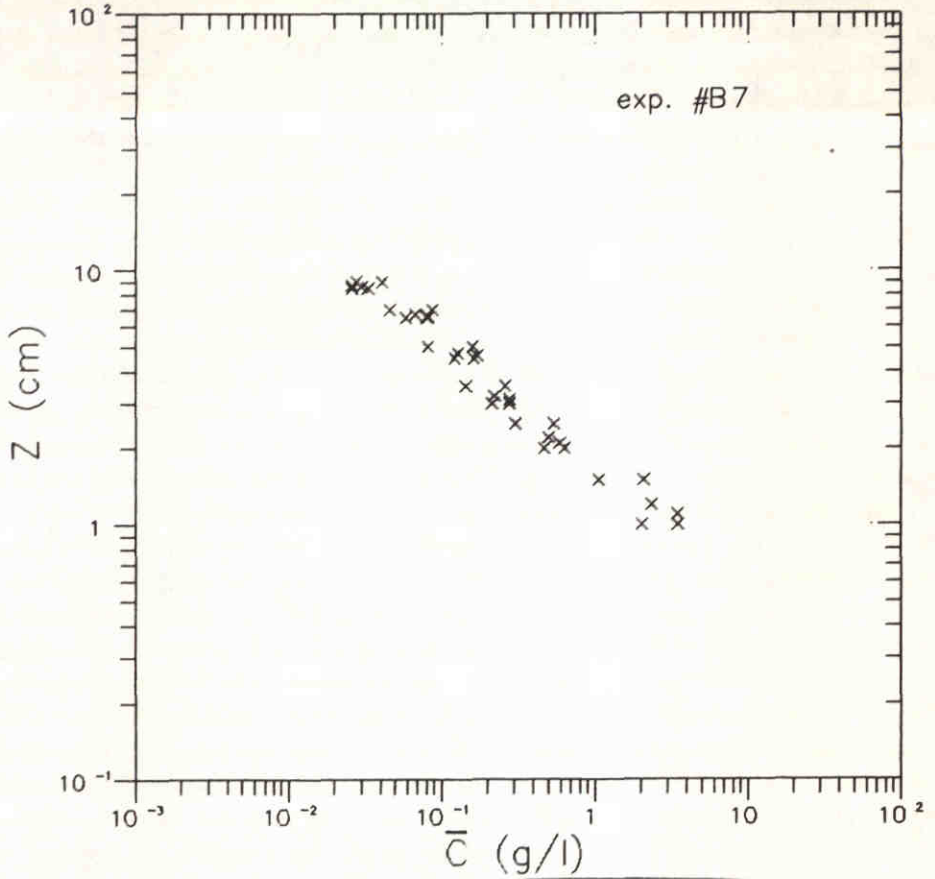

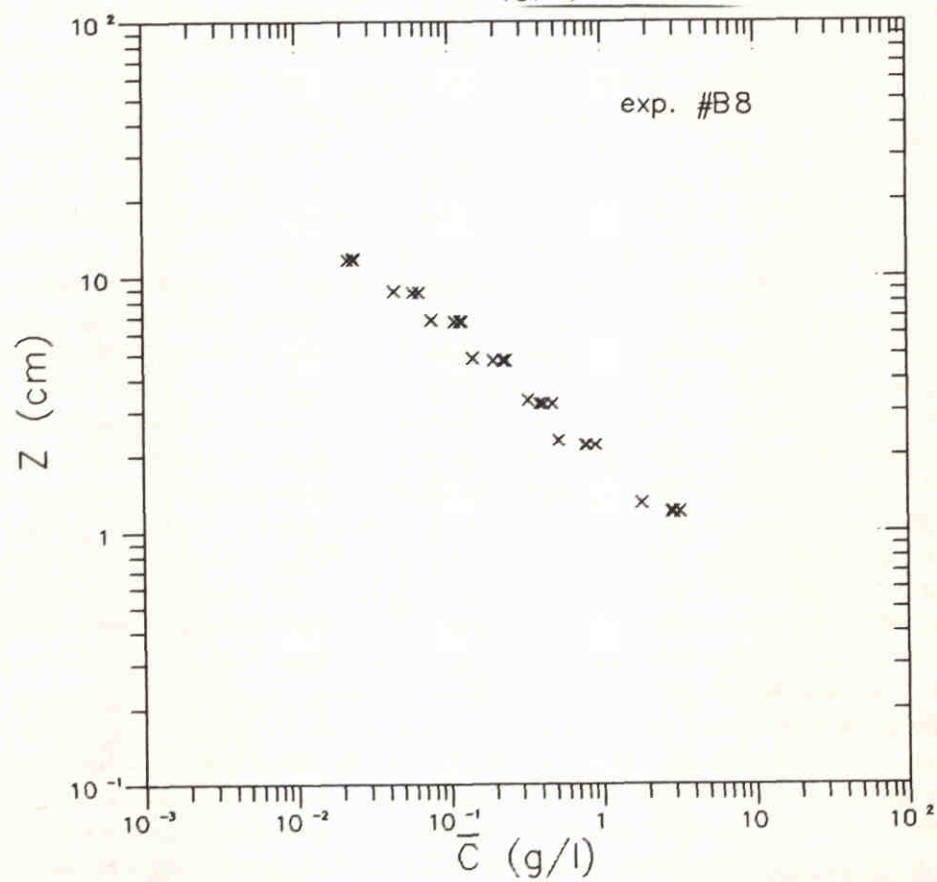

MEASURED TIME-AVERAGED CONCENTRATION PROFILES (LOG-LOG X-Y SCALES)

DELFT HYDRAULICS | H 840 | FIG. 3.16

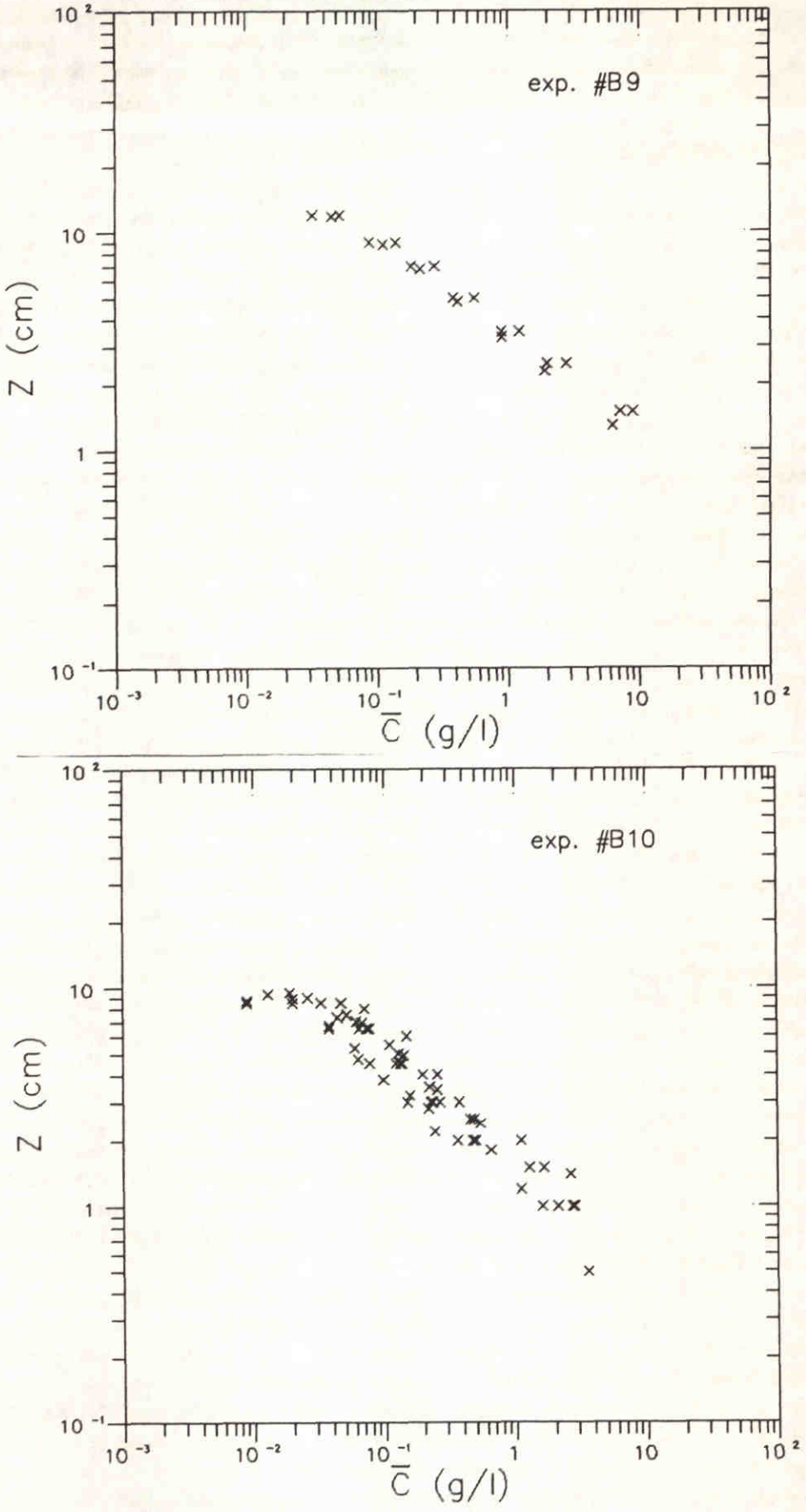

MEASURED TIME-AVERAGED CONCENTRATION PROFILES (LOG-LOG X-Y SCALES)

DELFT HYDRAULICS | H 840 | FIG. 3.17

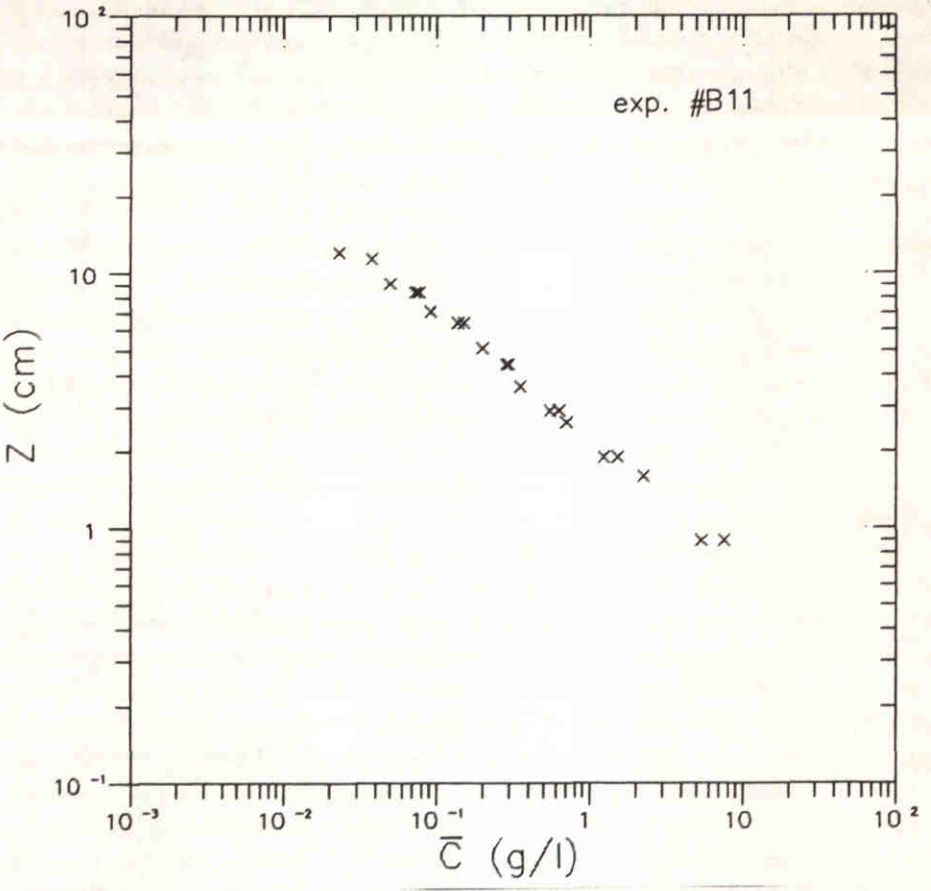

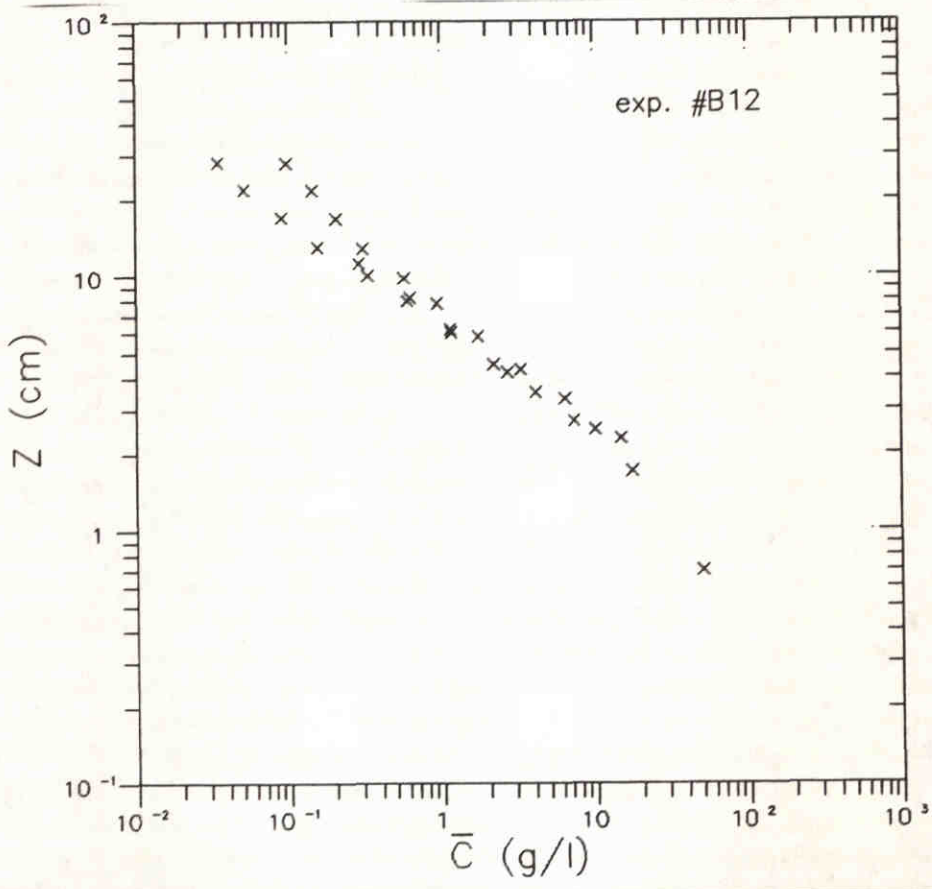

MEASURED TIME-AVERAGED CONCENTRATION PROFILES (LOG-LOG X-Y SCALES)

DELFT HYDRAULICS | H 840 | FIG. 3.18

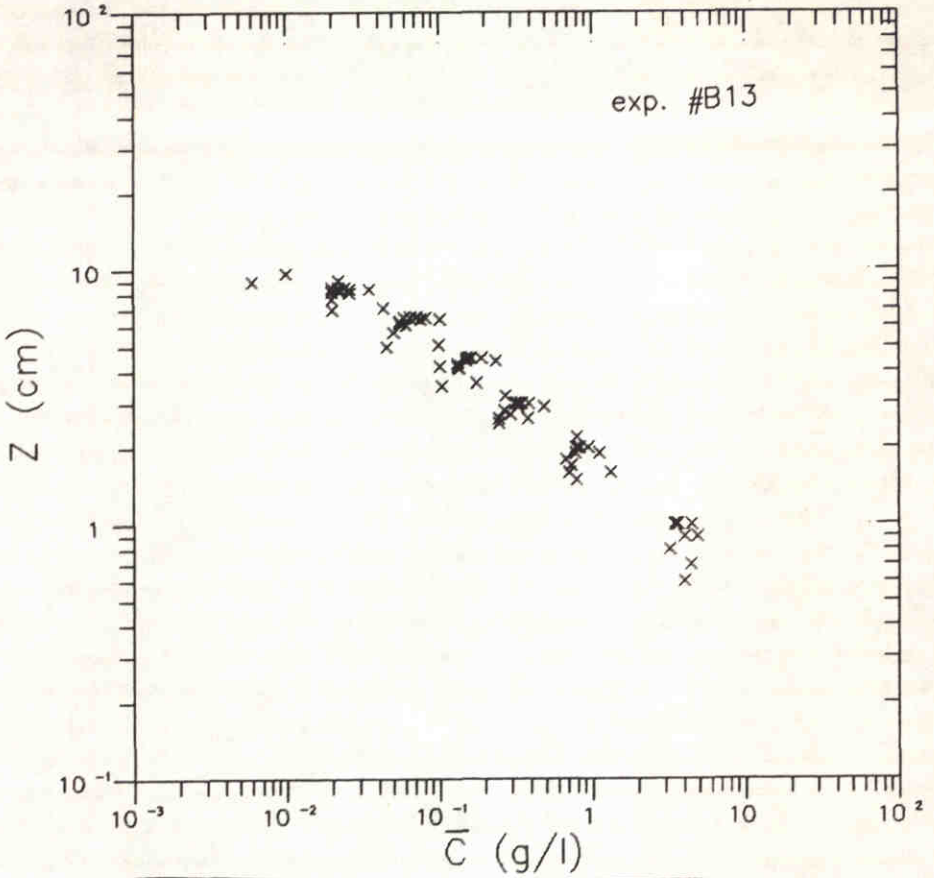

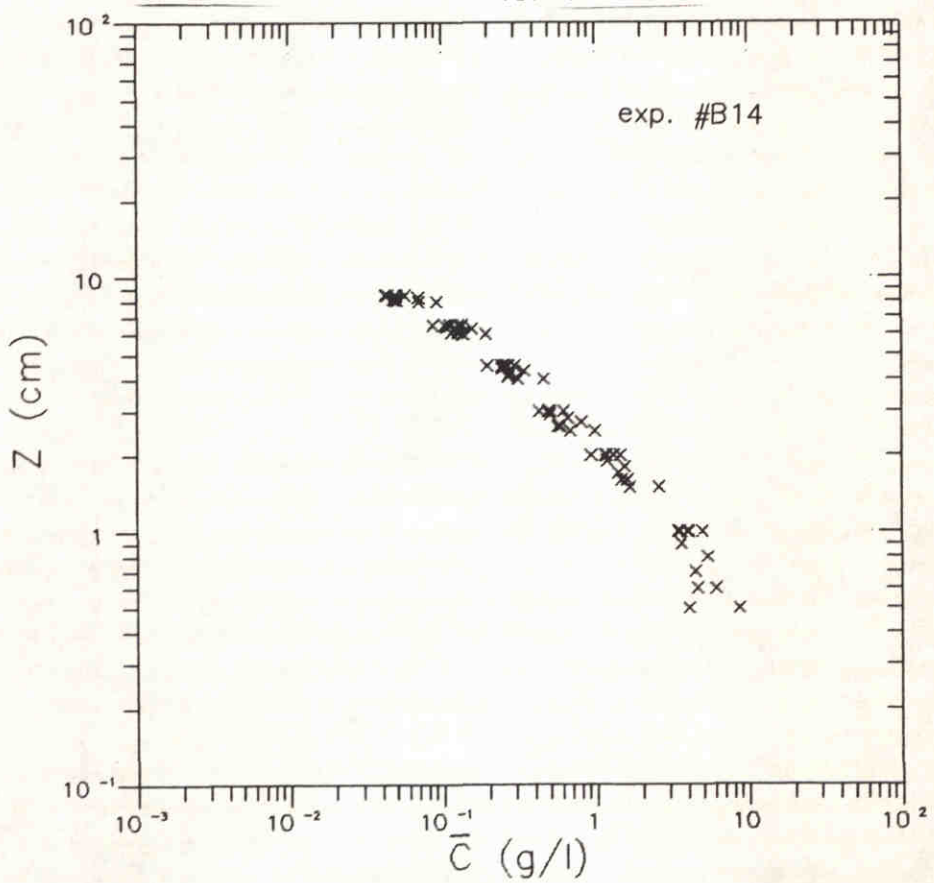

MEASURED TIME-AVERAGED CONCENTRATION PROFILES (LOG-LOG X-Y SCALES)

DELFT HYDRAULICS | H 840 | FIG. 3.19

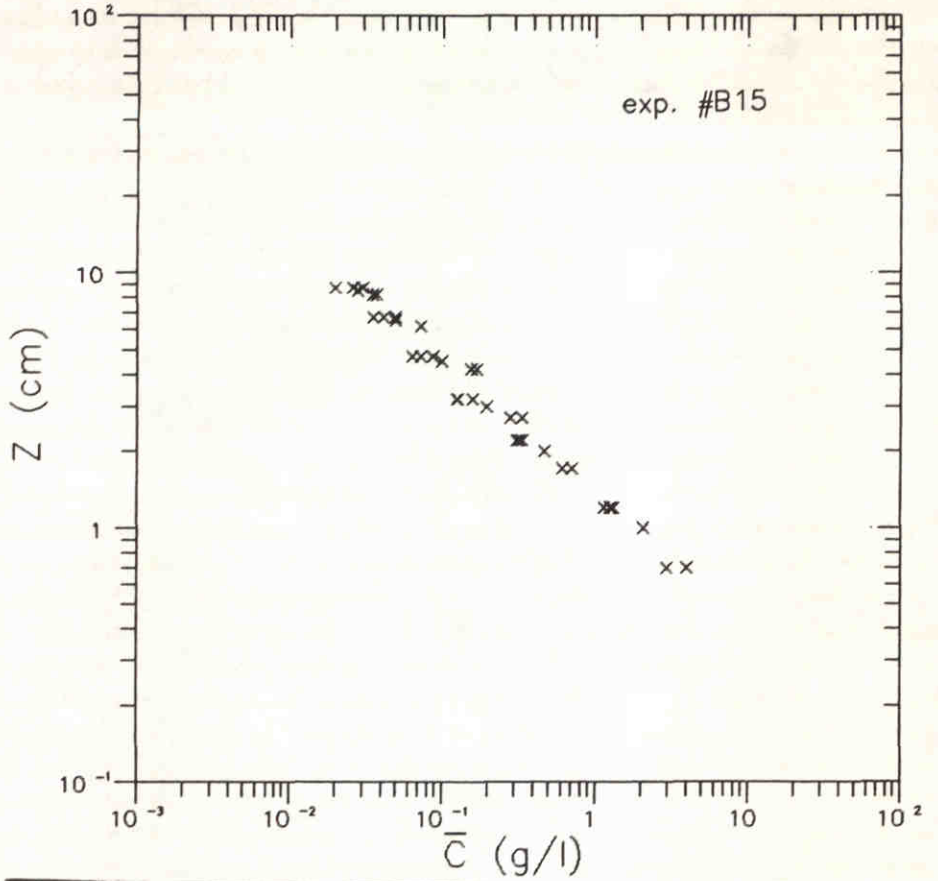

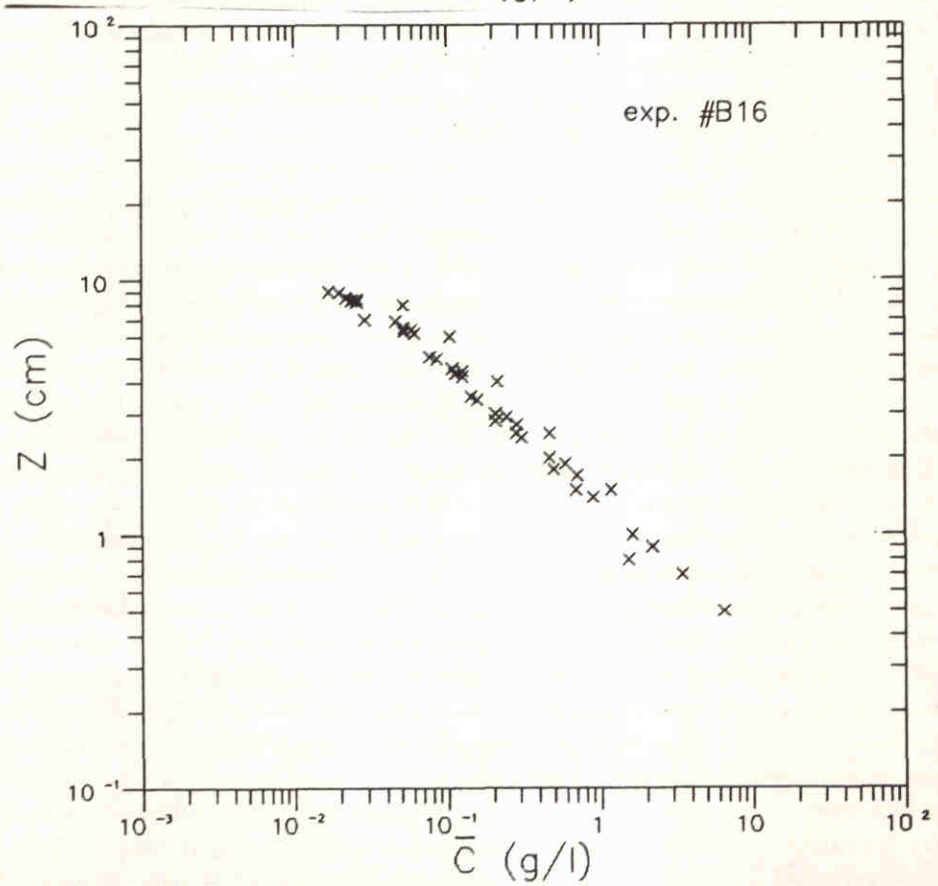

MEASURED TIME-AVERAGED CONCENTRATION PROFILES (LOG-LOG X-Y SCALES)

DELFT HYDRAULICS | H 840 | FIG. 3.20

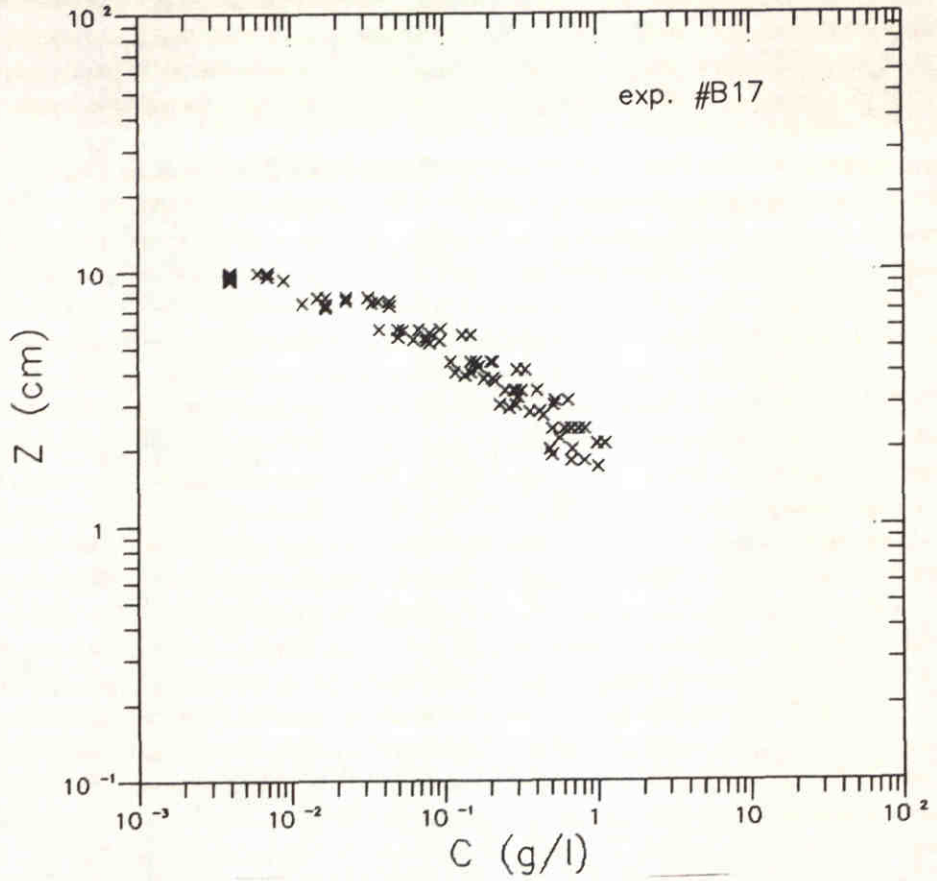

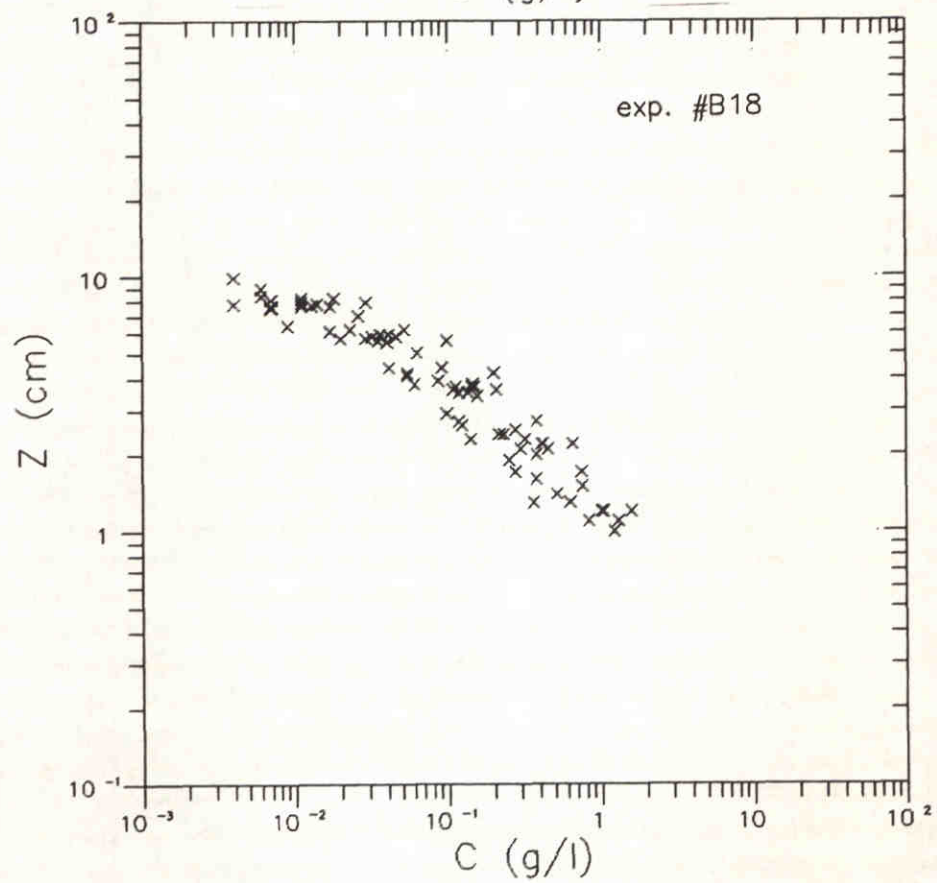

MEASURED TIME-AVERAGED CONCENTRATION PROFILES (LOG-LOG X-Y SCALES)

DELFT HYDRAULICS | H 840 | FIG. 3.21

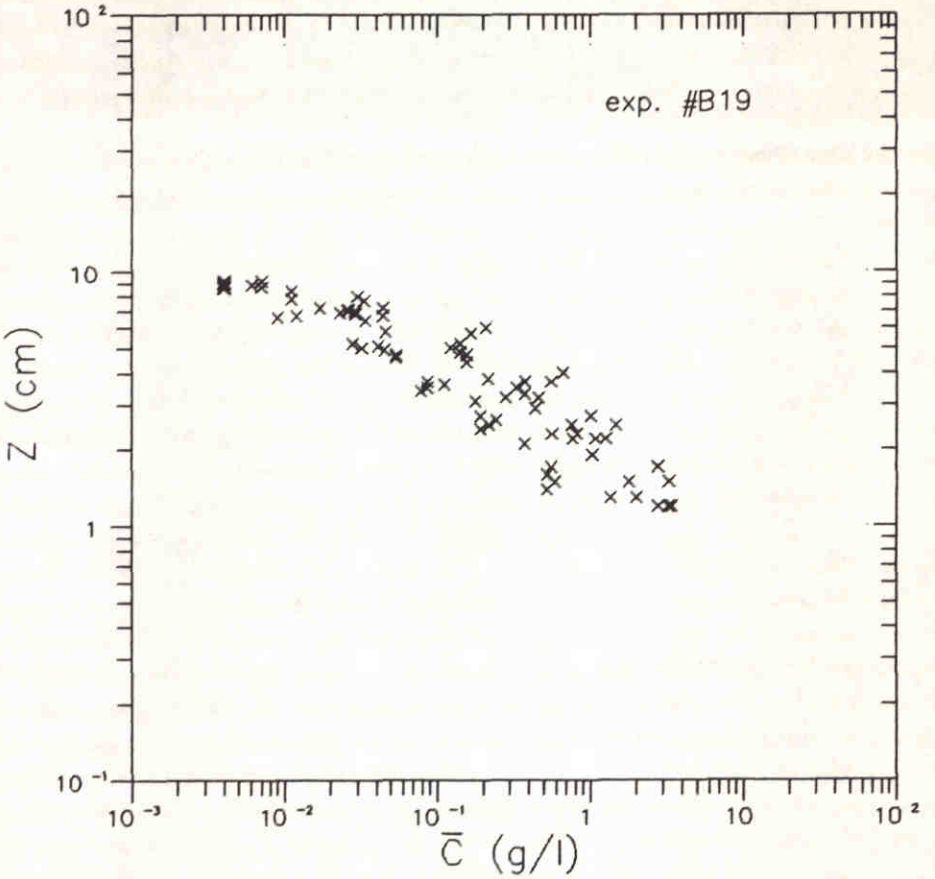

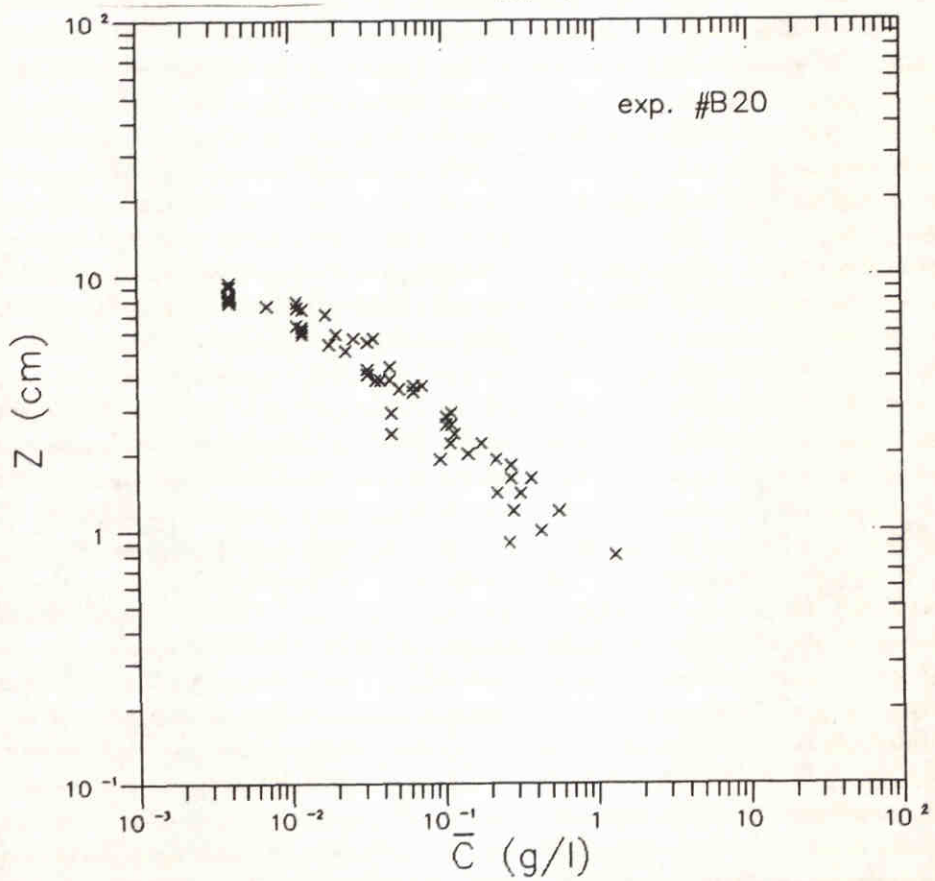

MEASURED TIME-AVERAGED CONCENTRATION PROFILES (LOG-LOG X-Y SCALES)

DELFT HYDRAULICS | H 840 | FIG. 3.22

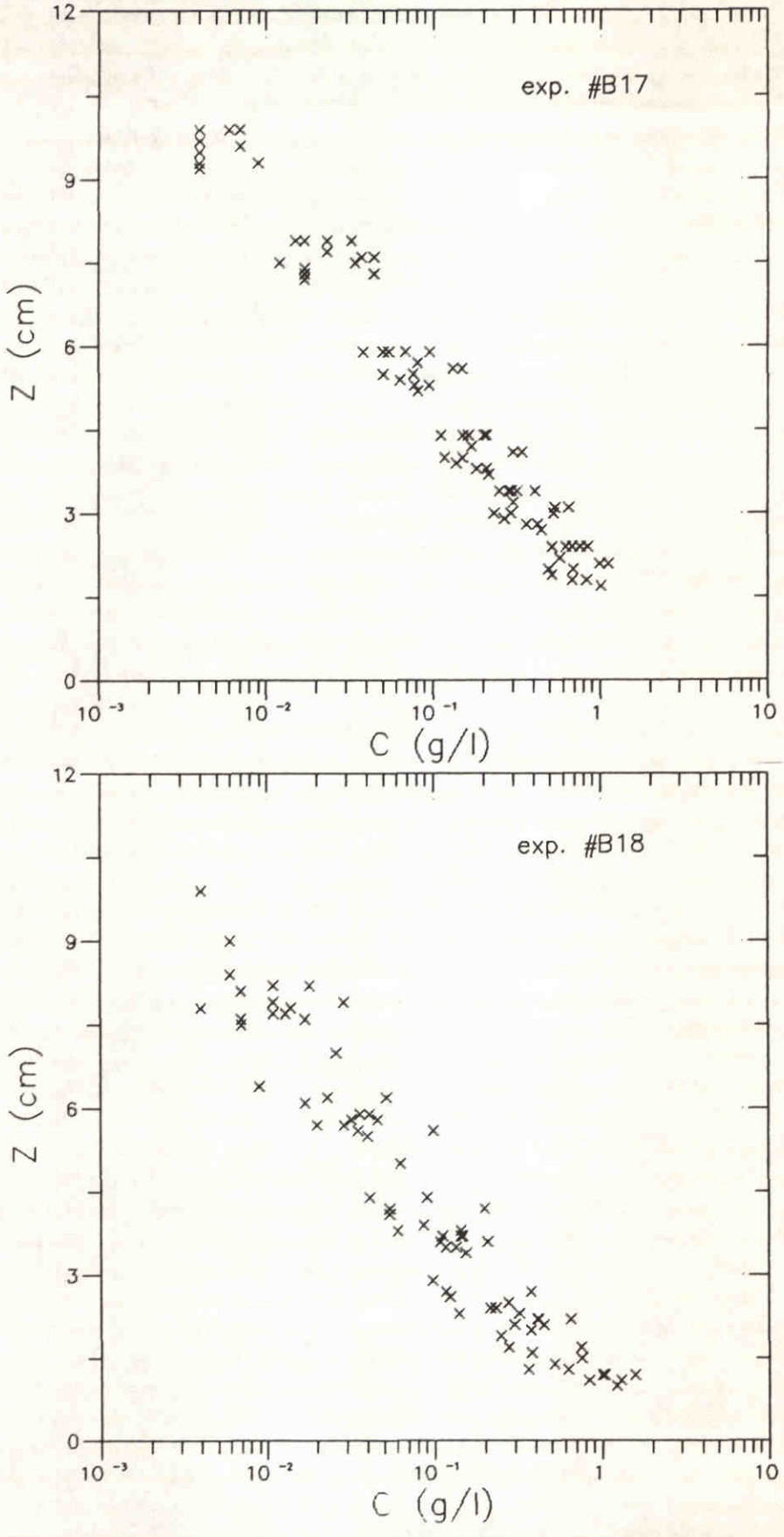

MEASURED TIME-AVERAGED CONCENTRATION PROFILES (LOG-LINEAR X-Y SCALES)

DELFT HYDRAULICS | H 840 | FIG. 3.23

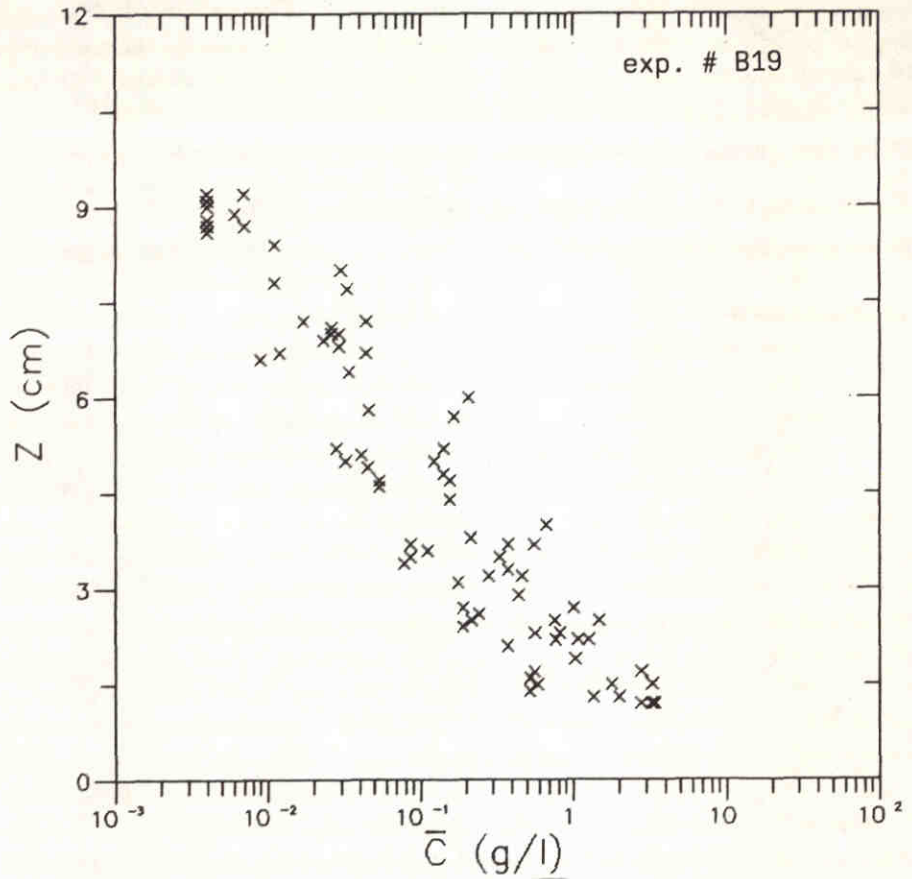

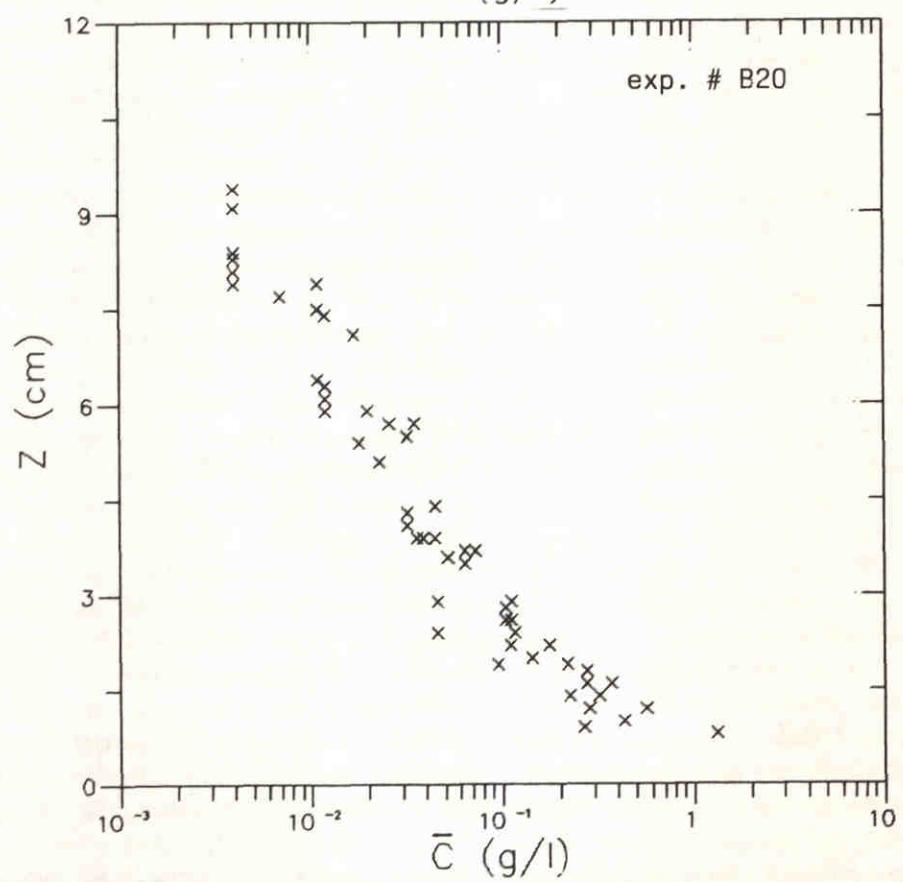

MEASURED TIME-AVERAGED CONCENTRATION PROFILES (LOG-LINEAR X-Y SCALES)

DELFT HYDRAULICS | H 840 | FIG. 3.24

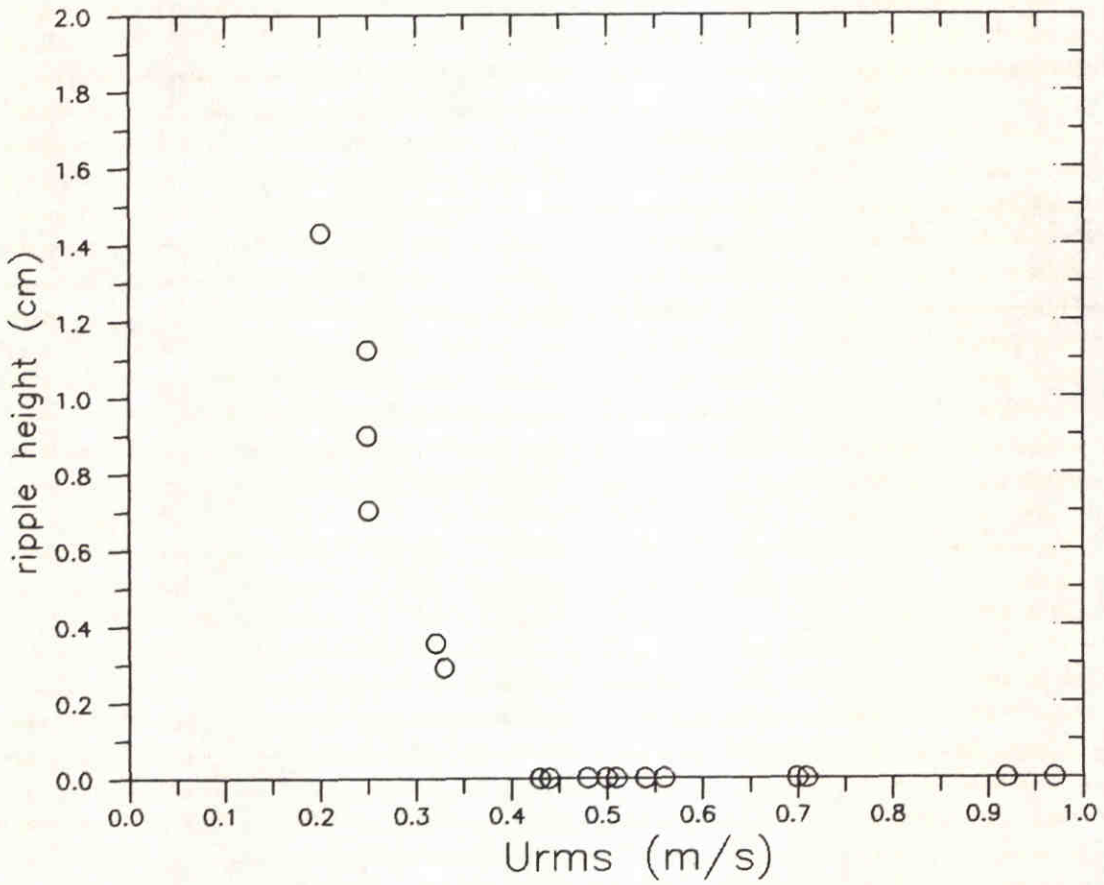

RIPPLE HEIGHT AS A FUNCTION OF U_{rms}

DELFT HYDRAULICS | H 840 | FIG. 3.25

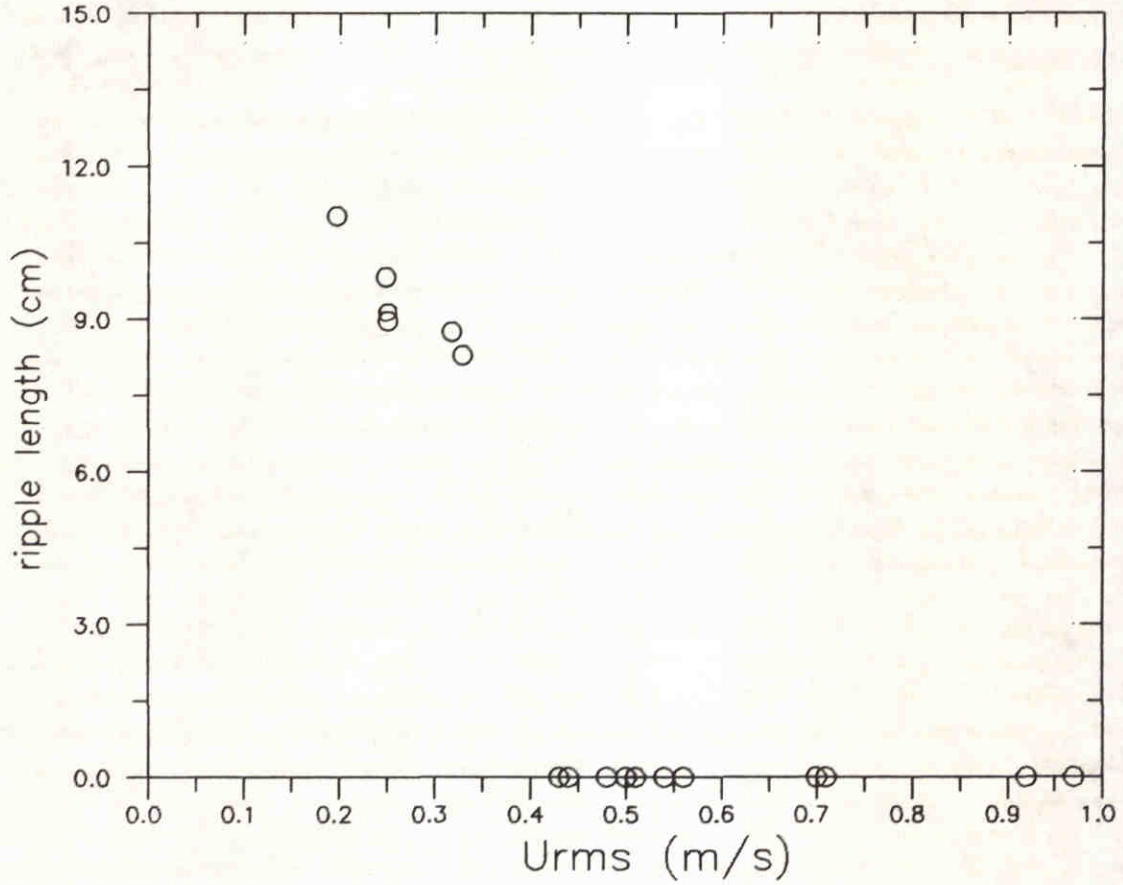

RIPPLE LENGTH AS A FUNCTION OF U_{rms}

DELFT HYDRAULICS | H 840 | FIG. 3.26

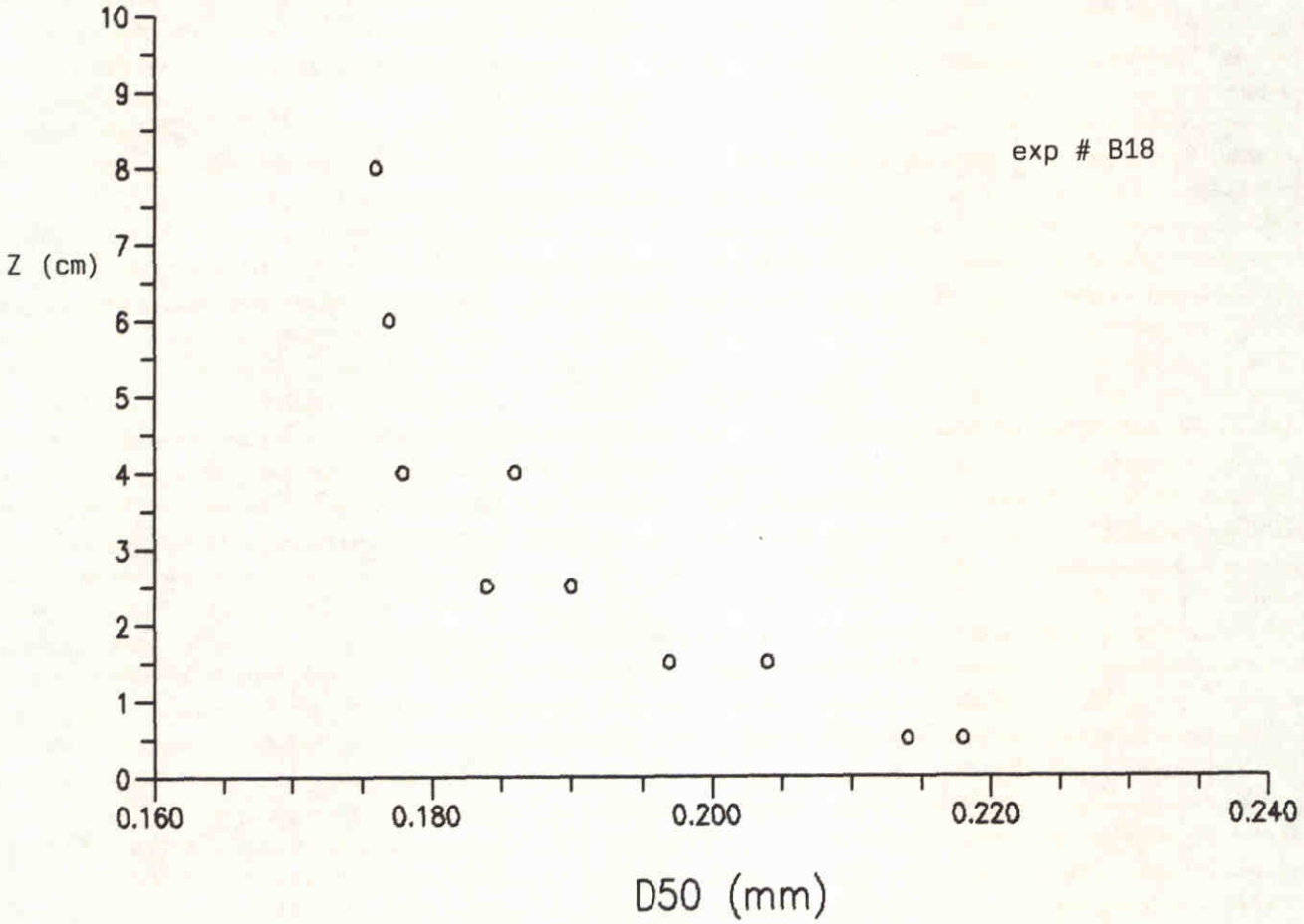

NON-UNIFORMITY OF SUSPENDED SEDIMENT (D50) ALONG THE VERTICAL PROFILE (VERTICAL SORTING)

DELFT HYDRAULICS | H 840 | FIG. 3.27

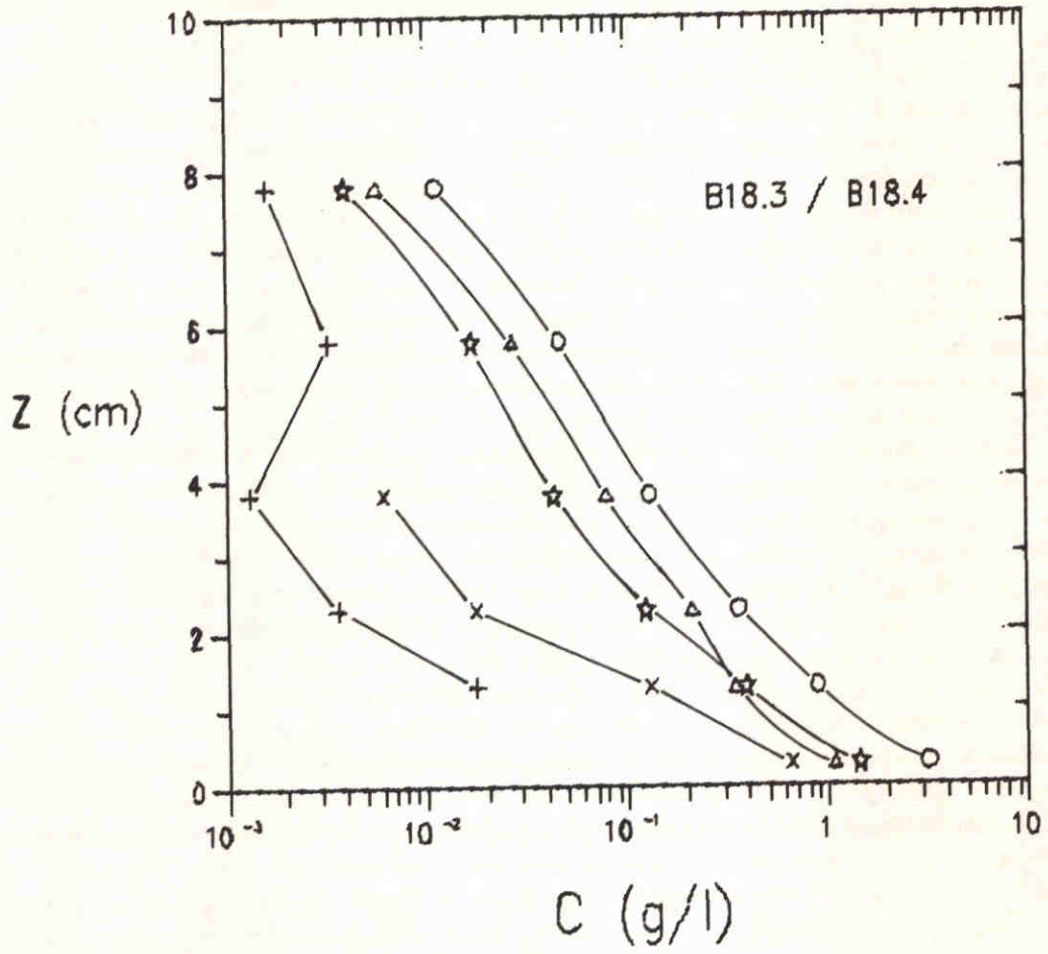

total	○
$0.10 < D_1 < 0.14$ mm	+
$0.14 < D_2 < 0.20$ mm	△
$0.20 < D_3 < 0.28$ mm	☆
$0.28 < D_4 < 0.40$ mm	×

MEASURED TIME-AVERAGED CONCENTRATION PROFILES OF INDIVIDUAL SIZE FRACTIONS (exp. B18)

DELFT HYDRAULICS | H 840 | FIG. 3.28

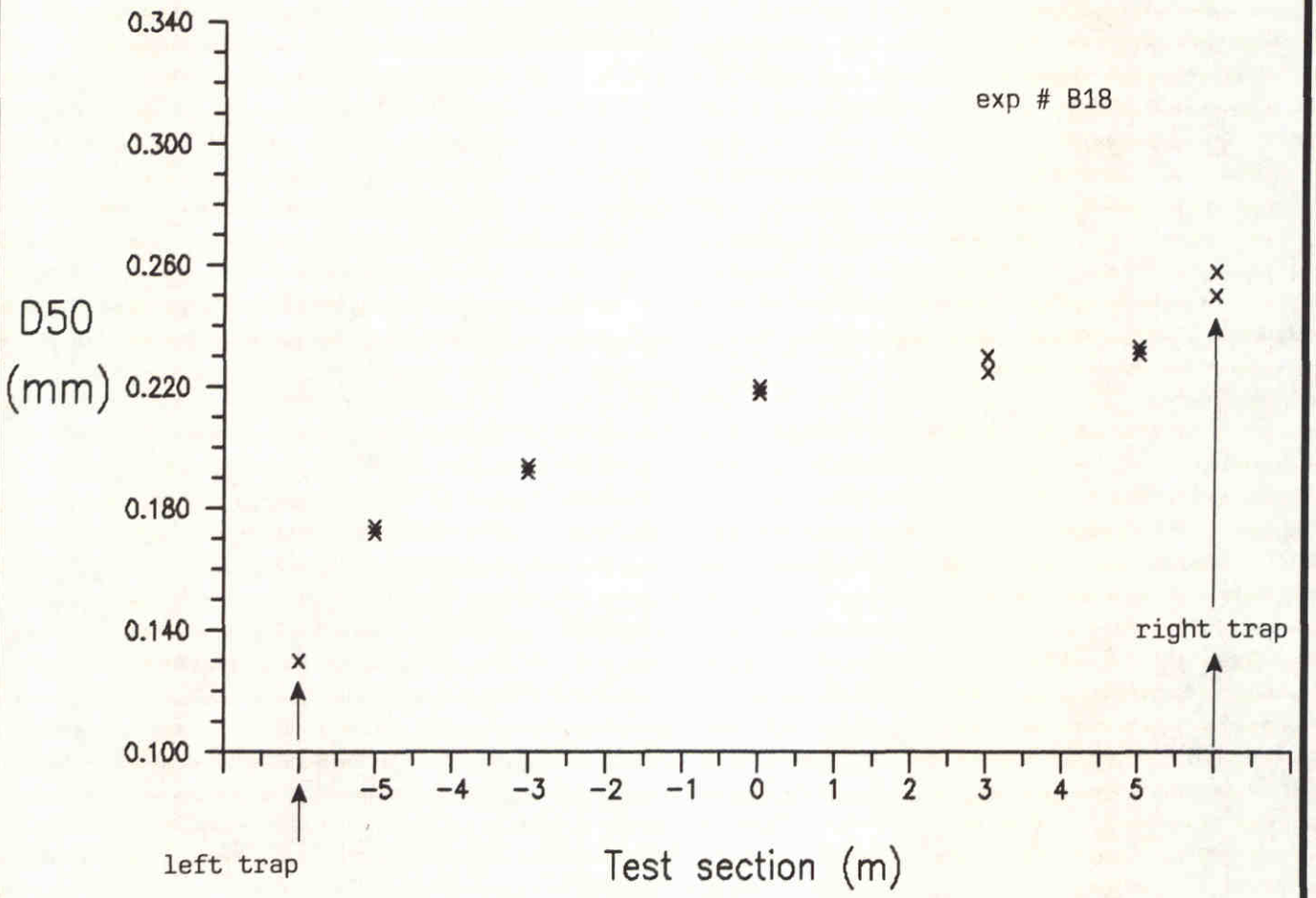

NON-UNIFORMITY OF THE BED MATERIAL (D50)
ALONG THE TEST SECTION (LONGITUDINAL SORTING)

DELFT HYDRAULICS | H 840 | FIG. 3.29

CURRENT-RELATED SEDIMENT FLUX PROFILES
(EXP'S B10, B17)

DELFT HYDRAULICS

H 840

FIG. 3.30

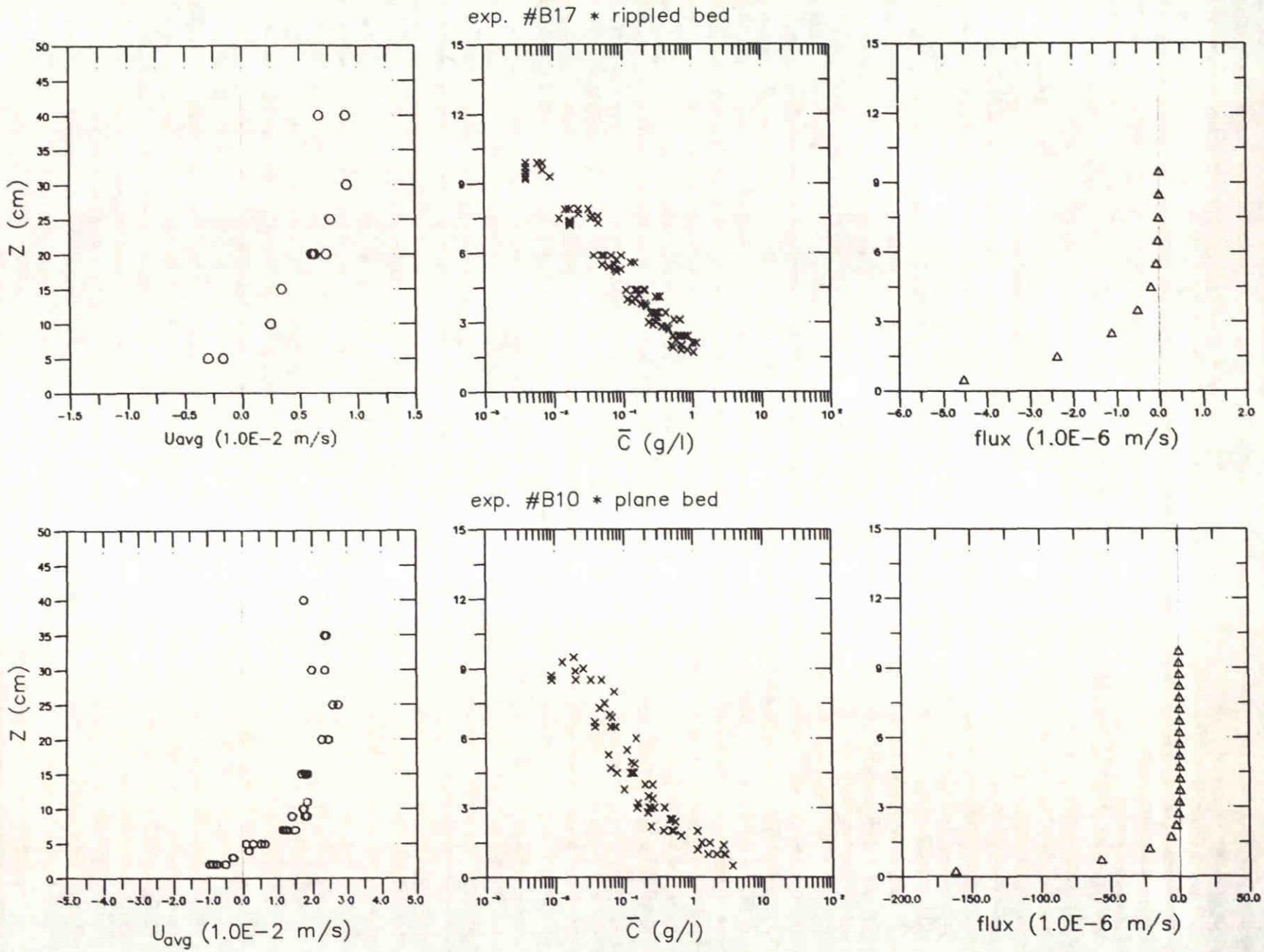

main office
Rotterdamseweg 185
p.o. box 177
2600 MH Delft
The Netherlands
telephone (31) 15 - 56 93 53
telefax (31) 15 - 61 96 74
telex 38176 hydel-nl

location 'De Voorst'
Voorsterweg 28, Marknesse
p.o. box 152
8300 AD Emmeloord
The Netherlands
telephone (31) 5274 - 29 22
telefax (31) 5274 - 35 73
telex 42290 hylvo-nl